MOLECULAR SIMULATION STUDIES OF MEA ABSORPTION PROCESS FOR CO_2 CAPTURE

LEE HON KIT

BACHELOR OF CHEMICAL ENGINEERING
UNIVERSITI MALAYSIA PAHANG

Thesis Access Form

No____________________________Location______________________________

Author : LEE HON KIT

Title : MOLECULAR SIMULATION STUDIES OF MEA ABSORPTION PROCESS FOR CO2 CAPTURE

Status of access OPEN / RESTRICTED / CONFIDENTIAL

Moratorium period:______________ years, ending___________/_______200____

Conditions of access proved by (CAPITALS): DR NOORLISA BINTI HARUN

Supervisor (Signature)………………………………………………

Faculty: Faculty of Chemical & Natural Resources Engineering

Author’s Declaration: *I agree the following conditions:*

OPEN access work shall be made available in the Universiti Malaysia Pahang only and not allowed to reproduce for any purposes.

The statement itself shall apply to ***ALL*** *copies:*

This copy has been supplied on the understanding that it is copyright material and that no quotation from the thesis may be published without proper acknowledgement.

Restricted/confidential work: All access and any photocopying shall be strictly subject to written permission from the University Head of Department and any external sponsor, if any.

Author's signature……………………………………….Date: ………………………………

users declaration: for signature during any Moratorium period (Not Open work): ***I undertake to uphold the above conditions:***

Date	Name (CAPITALS)	Signature	Address

MOLECULAR SIMULATION STUDIES OF MEA ABSORPTION PROCESS FOR CO_2 CAPTURE

LEE HON KIT

Thesis submitted in partial fulfilment of the requirements
For the award of the degree of
Bachelor of Chemical Engineering

Faculty of Chemical & Natural Resources Engineering
UNIVERSITI MALAYSIA PAHANG

JANUARY 2015

SUPERVISOR’S DECLARATION

We hereby declare that we have checked this thesis and in our opinion, this thesis is adequate in terms of scope and quality for the award of the degree of Bachelor of Chemical Engineering.

Signature :
Name of main supervisor : DR. NOORLISA BINTI HARUN
Position : SENIOR LECTURER
Date :

STUDENT'S DECLARATION

I hereby declare that the work in this thesis is my own except for quotations and summaries which have been duly acknowledged. The thesis has not been accepted for any degree and is not concurrently submitted for award of other degree.

Signature :
Name : LEE HON KIT
ID Number : KA11182
Date : JANUARY 2015

Dedication

I dedicate my dissertation work to my family and all friends. I would like to dedicate this thesis and everything I do to my loving parents, Lee Tee Min and Khong Yit Mei whose give the words of encouragement and push for tenacity ring in my ears. Both of you have been my best cheerleaders. I also dedicate this dissertation to my friends and supervisors who have supported me throughout the process.

ACKNOWLEDGEMENT

I would like to thank the following people and organizations;

- My supervisors Dr. Noorlisa binti Harun and Kak Emyra for their guidance through an effective well-arranged weekly meeting, helping me in understanding my project title, and advising me during completing this research and writing the dissertation.
- Meanwhile, thanks to Kak Hana for the guidance all the ways during simulation process.

ABSTRACT

Concentration of CO_2 in the atmosphere is increasing rapidly. Emission of CO_2 directly impact on global climate change. Monoethanolamine (MEA) absorption process for CO_2 capture was developed to combat this trend due to its high reactivity. This allows higher priority absorption for carbon dioxide. The aim of this study is to investigate the intermolecular interaction between the solvent (MEA) and the acid gas (CO_2) during the absorption process. Molecular dynamic (MD) simulation will be used to study the molecular interaction and give insight of this process at molecular level. The intermolecular interactions for pure molecules (pure MEA, pure water, and pure CO2), binary system (MEA+CO2, CO2+H2O and MEA+H2O) and tertiary system (MEA+CO2+H2O) at different operating conditions are considered in this study. To perform the molecular dynamic (MD) simulation two boxes of carbon dioxide gas and MEA solvent are combined to study the absorption process. Thermodynamic condition under NVE, NPT and NVT conditions is specified in the simulation. The simulation results are analysed in terms of radical distribution function (rdf) to describe the intermolecular interaction and diffusion coefficient to calculate the solubility factor. Meanwhile, Mean square displacement (MSD) is also used to determine the diffusivity of molecules. The rdf function is plotted on the graph to identify the highest potential molecular interaction at various operating conditions. MD simulation was performed at temperature of 25^oC, 40^oC, and 45^oC to observe the potential interaction of molecules. The trend of rdf graph of each component shows an increasing trend with increase temperature. The purpose of studying primary system is to study the intermolecular interaction of each component on effects of different temperature. A further analysis of binary system was performed to study the intermolecular interaction between MEA molecule and H_2O molecule. The rdf graph generated from simulation proved that solubility of MEA in water increase with temperature. Hydroxyl group, –OH of MEA molecule interact with water to form hydrogen bonding bond. Tertiary system of intermolecular interaction is performed to study the CO_2 absorption in aqueous MEA solution. It is found that the amine group, -NH of MEA has higher probability to form carbamate ion with carbon dioxide compare to –OH group of MEA. As a references from binary system for tertiary system, higher number of lone pairs in hydroxyl group than amine group of MEA tends to form hydrogen bonds with water.

ABSTRAK

Kepekatan CO_2 dalam atmosfera meningkat dengan cepat. Pelepasan CO_2 memberi kesan secara langsung ke atas perubahan iklim global. Monoethanolamine (MEA) proses penyerapan untuk pengumpulan CO2 telah dijalankan untuk memerangi trend ini kerana kereaktifan yang tinggi. Ini membolehkan penyerapan yang lebih tinggi untuk karbon dioksida. Tujuan kajian ini adalah untuk menyiasat interaksi antara molekul antara pelarut (MEA) dan gas asid (CO2) semasa proses penyerapan. Molekul dinamik (MD) simulasi akan digunakan untuk mengkaji interaksi molekul dan memberikan wawasan proses ini pada peringkat molekul. Interaksi antara molekul bagi molekul tulen (MEA tulen, air tulen, dan CO2 tulen), sistem binari (MEA + CO2, CO2 + H2O dan MEA + H2O) dan sistem ketiga (MEA + CO2 + H2O) pada keadaan operasi yang berbeza dipertimbangkan dalam kajian ini. Untuk melaksanakan dinamik molekul (MD) simulasi dua kotak gas karbon dioksida dan MEA pelarut digabungkan untuk mengkaji proses penyerapan. Keadaan termodinamik bawah NVE, NPT dan NVT syarat yang dinyatakan dalam penyelakuan. Keputusan simulasi dianalisis dari segi fungsi taburan radikal (RDF) untuk menerangkan interaksi antara molekul dan resapan pekali untuk mengira faktor kelarutan. Sementara itu, Mean square displacement (MSD) juga digunakan untuk menentukan kemeresapan molekul. Fungsi RDF diplotkan pada graf untuk mengenalpasti interaksi tertinggi potensi molekul di pelbagai keadaan operasi. MD simulasi telah dilakukan pada suhu 25^oC, 40^oC dan 45^oC untuk memerhati interaksi potensi molekul. Trend graf RDF setiap komponen menunjukkan trend yang meningkat dengan peningkatan suhu. Tujuan belajar sistem pertama adalah untuk mengkaji interaksi antara molekul setiap komponen pada kesan suhu yang berbeza. Secara lebih terperinci sistem binari telah dijalankan untuk mengkaji interaksi antara molekul antara molekul MEA dan molekul H_2O. Graf RDF dihasilkan daripada simulasi membuktikan bahawa kelarutan MEA dalam air meningkat dengan suhu. Kumpulan hidroksil, -OH molekul MEA berinteraksi dengan air untuk membentuk hidrogen bon ikatan. Sistem ketiga dijalankan untuk mengkaji penyerapan CO_2 dalam larutan akueus MEA. Ia didapati bahawa kumpulan amina yang, -NH daripada MEA mempunyai kebarangkalian yang lebih tinggi untuk membentuk ion karbamat dengan karbon dioksida berbanding dengan kumpulan -OH MEA. Sebagai rujukan dari sistem binari untuk sistem ketiga, jumlah yang lebih tinggi daripada pasangan tunggal dalam kumpulan hidroksil daripada kumpulan amina daripada MEA cenderung untuk membentuk ikatan hidrogen dengan air.

TABLE OF CONTENTS

LIST OF FIGURES

LIST OF TABLES

LIST OF ABBREVIATIONS

a_i	Acceleration
ε_o	Vacuum permittivity
ε_T	Relative permittivity
f_i	Force of Newton's second law of motion
m_i	Mass of particle
ρ	Density of atoms
r	Spherical radius
r_i	Change in particle position
$V(r_i)$	Potential energy respect to particle position
t	Time
∇_i	3 dimensions
Φ	Harmonic interaction force
Ψ_{nlm_l}	Wave function

Greek

Å	Amstrong
E	Energy
K	Harmonic force constant
M	Diffusion coefficient
N	Number of mole
N_i	atomic population
P	Pressure
P_{ii}	density matrix
S_{ii}	overlap matrix
T	Temperature
U_{AB}	Potential Energy
V	Volume

LIST OF ABBREVIATIONS

AO	Atomic orbitals
EIA	Energy information administration
DEA	Diethanolamine
MEA	Monoethanolamine
MD	Molecular dynamics simulation
MDEA	Methyldiethanolamine
MM	Molecular mechanic
MO	Molecular wave functions
MPA	Mulliken population analysis
MSD	Mean square displacement
QM	Quantum mechanic
RDF	radial distribution function
COMPASS	Condensed-phase optimized molecular potentials for atomic simulation studies
NPT	Constant number of moles, pressures and temperatures
NVE	Constant number of moles, volumes and energies
NVT	Constant number of moles, volumes and temperatures
LJ	Lernnard Jones potential
LPA	Löwdin population analysis
PBC	Periodic boundry condition (PBC)

1 INTRODUCTION

1.1 *Motivation and statement of problem*

Carbon dioxide is a well-known gases that are found everywhere in the atmosphere. In other country such as Canada and United State of America, greenhouse gas mitigation technology was introduced particularly with respect to increasing carbon dioxide in the light of climate change fears due to human activities (Rubin & De Coninck, 2005). Figure 1-1 shows the rise in global mean surface temperature and average temperature from 1961 – 1990 (Wessner, 2009). For the past 30 years, the growing in the concentration of carbon dioxide in atmosphere literally increases with the global temperature.

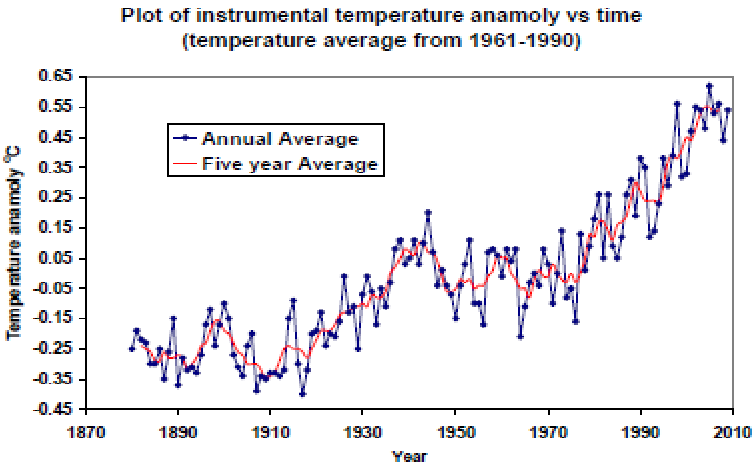

Figure 1-1: Plot of instrumental temperature anomaly versus time (temperature average from 1961 – 1990).

In US, 98% of greenhouse emissions is carbon dioxide in 2007, 40% is from electricity generation (Energy Information Administration, 2007). Most electricity generating sector such as fossil fuel power plant creates concentrated and large amount of carbon dioxide gas. The emissions of carbon dioxide in 2013 are about 32.5 billion metric tons. Energy Information Administration (EIA) estimates that the emissions of carbon dioxide will increase from 31 billion metric tons in 2010 to 36 billion metric tons in 2020, a 1.6% increase in every year (Energy Information Administration, 2013). Hence, there is an urgent need to deploy technologies that can utilize the fossil fuels in a cleaner way (less carbon dioxide released) to provide a bridge to a greener economy in the future. MEA absorption process for carbon dioxide removal is the most promising technology available to stabilize the global climate change due to CO_2 emissions (Anusha, 2010).

1.2 Objectives

This research project aims to:

- Study the intermolecular interaction in monoethanolamine absorption process for carbon dioxide capture via molecular dynamic simulation technique at different process operating condition. The strength of intermolecular interaction between the CO_2 and the solvent will represent the absorption effectiveness.

1.3 Scope of this research

This case study cover few scopes,

- Molecular Dynamic (MD) simulation was used to study and give insight on the intermolecular interaction between solvent and acid gases in the absorption process.
- There are different systems at various operating conditions are considered in this study; pure molecules (pure MEA, pure water, and pure CO_2), binary system (MEA+CO_2, CO_2+H_2O and MEA+H_2O) and tertiary system (MEA+CO_2+H_2O).
- The optimum molecular interaction will be determined by observing the highest intermolecular interaction between molecular while simulating the absorption process at different temperature.
- Monoethanolamine act as the solvent while carbon dioxide is the acid gas. Since monoethanolamine is a primary amines and it is more effective for carbon dioxide removal compared to secondary and tertiary amines. It will form carbamate ions during the absorption process (Rajesh et al. 2006). The equation is:

$$HOC_2H_4NH_2 + CO_2 \leftrightarrow HOC_2H_4NH_3^+ + HOC_2H_4NCOO^- \quad \text{(carbamate)}$$

The molecule interaction between MEA and carbon dioxide during the absorption process to form carbamate ion will be analysed and study through radial distribution function (rdf) graph.

- Mean square displacement is used to calculate the diffusion coefficient.

1.4 Main contribution of this work

This study gives insight on the molecular interaction between carbon dioxide and monoethanolamine during the absorption process. Meanwhile, the maximum intermolecular interaction occurred during the absorption process will be determined at various operating conditions.

1.5 Organisation of this thesis

The structure of the thesis is outlined as follow:

Chapter 2 presents the reviews of open literature of published researches which have been conducted in this regard. Brief explanation on amine based absorption process for carbon dioxide and reactivity of different types of alkanolamines is included in this chapter. The intermolecular interactions involved during the simulations and the thermodynamic properties used in this study also clearly explained in this chapter.

Chapter 3 describes the methodology applied in this study which includes the procedure and force fields specified in the simulation process. This chapter also explain the method to interpret radical distribution function into graphical form to analyse the intermolecular interaction between atoms.

Chapter 4 discuss the results obtained from the simulation. The results are interpreted to give insight on how the intermolecular interaction obtained from the molecular dynamic simulation will explain absorption process at molecular level.

Chapter 5 draws the summary of thesis and outlines the future work which might be derived from the model developed in this work.

2 LITERATURE REVIEW

2.1 Introduction

This chapter discusses the carbon dioxide separation technologies, amine based absorption process, molecular dynamic simulation (MD) and modeling of molecules. The aim of this chapter is to review the fundamental science of the absorption process and the simulation technique.

2.2 Carbon dioxide separation technologies

There are several technologies available for carbon dioxide capture such as adsorption, membrane separation, cryogenic separation, physical and chemical absorption (Rackley, 2010). According to Zakkour and Cook 2010,

a) Membrane separation: Application of membrane separation typically a permeation process where carbon dioxide is absorbed into the membrane using polymer-based membranes, metallic membranes or ceramic membranes, then diffuse through it. In all cases, the pressure different across the membrane critically induce the flow across the membrane. So, membrane separation seldom uses for carbon dioxide capturing from flue gas which contained low CO_2 concentration and at low pressure.

b) Chemical solvents: Through this process, gas mixture is contacted with chemical solvent such as amines and alkanolamines in absorption tower. Most chemical solvent especially amines such as monoethanolamine (MEA) with smaller plant size is able to remove carbon dioxide at low concentrations and make the process suitable for low pressure, low carbon dioxide concentrations gas stream (Sada, Kumazawa, & Butt, 1976).

c) Physical sorbents: This process similar to chemical sorbent but the different is the way to absorb carbon dioxide as it utilize weak physical bond as opposed to chemical bonds used for chemical solvents. Zeolites and activated carbon are some of the examples of solid adsorbent used to separate carbon dioxide from gas mixtures (Young & Crowell, 1962).

d) Cryogenic separation process: The process involves using of distillation column which gas mixture is introduced at the based then it migrates up through the column. Various fractions are then separate at different heights and dew points. High purity of carbon dioxide can be achieved using this technique but cryogenic separation technique has not achieved widespread commercial development (Jha, 2006).

2.3 Amine based absorption process

2.3.1 Process

There are many ways to capture carbon dioxide as previously mention. In this study, chemical solvent separation technology using monoethanolamine was selected since amine based absorption is more effective for carbon dioxide removal from flue gas (Chakrawarti et al., 2001).

This process involved a reversible reaction between a weak acid (CO_2) and a weak base (MEA) to form a soluble salt. Figure 2-1 shows the process flow diagram of the MEA based absorption process. In absorber, the inlet carbon dioxide is absorbed by the MEA. The solution enriched with CO_2 is then preheated before entering the stripper. After addition of heat, the reaction is reversed. From the bottom of the column, heat exchanges occur between the solvents and recycle back to the absorber. From the top, a high purity of carbon dioxide is produced (Alie, 2004).

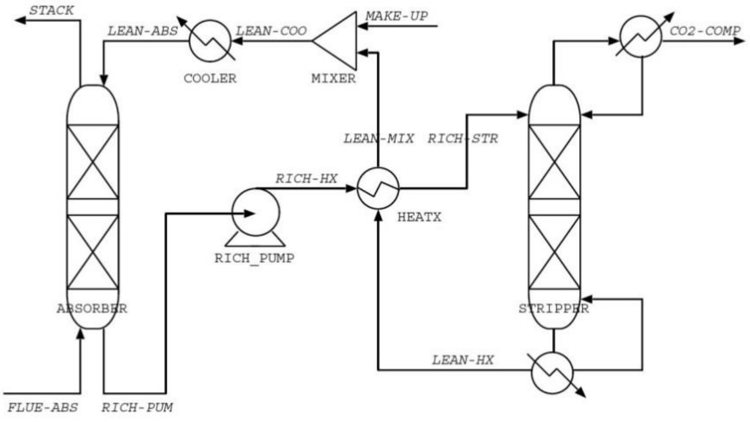

Figure 2-1: Process flow diagram for CO2 removal via chemical absorption

The advantage of amine based adsorption technology is it is a matured technology for carbon dioxide capture and has been used for many oil and gas industries. It is suitable for retrofitting of the existing power plants (Yu & Huang et al., 2012). Amine based absorption have alkanoamines which containing at least one hydroxyl group. It also helps to reduce vapor pressure and increase their solubility in aqueous solution (Park & Yoon et al., 2006).

2.3.2 Categorization of Alkanolamines

According to Farmahini 2010, alkanolamines are considering in group of ammonia derivatives which consists of at least one hydroxyl group and one amine group. The amine group can be classified into three subcategories based on the number of substituents on the nitrogen atom. The three classes of alkanolamines are as as described:

a) Primary alkanolamines: The amine carries one ethanol group and two hydrogen atoms are directly bonded to the nitrogen atom. Monoethanolamine (MEA) is an example of this category.

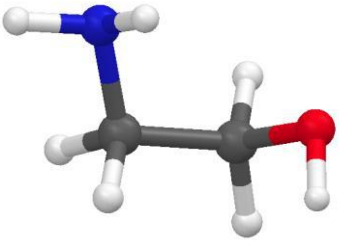

Figure 2-2: Molecular structure of monoethanolamine, C_2H_7NO

b) Secondary alkanolamines: In this category, each hydrogen from both side ends of the amine group has been replaced by ethanol group and only one hydrogen atom attached to the nitrogen atom. The best example is diethanolamine (DEA).

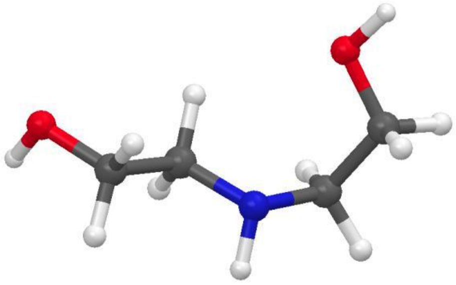

Figure 2-3: Molecular structure of diethanolamine, $C_4H_{11}NO_2$

c) Tertiary alkanolamines: These alkanolamines have one ethanol group at both end sides and no hydrogen bonded to the nitrogen atom. The hydrogen atoms have replaced by substituent groups which is the alkyl or alkanol groups. The best example is the methyldiethanolamine (MDEA).

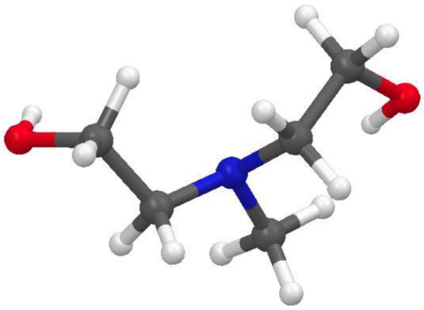

Figure 2-4: Molecular structure of methyldiethanolamine, $CH_3N(C_2H_4OH)_2$

2.3.3 *Reaction between Amines and CO_2*

Amine based absorption process technology is used to capture CO_2 in a large scale with amines as the solvent. There are three main type of amines can be used in absorption process. The three main types are primary amines (MEA), secondary amines (DEA) and tertiary amines (MDEA) (Nathalic et al., 2012).

The reaction between primary and secondary amines with CO_2 will form carbamate ion. Where else tertiary amines will form bicarbamate when react with CO_2. The reactions during the absorption process can be expressed as follows:

Primary or Secondary amines,

$$2R_1R_2NH + CO_2 \leftrightarrow R_1R_2NH^+ + R_1R_2NCOO^- \ (carbamate) \tag{2.1}$$

Tertiary amines,

$$R_1R_2NH + H_2O + CO_2 \leftrightarrow R_1R_2NH^+ + HCO_3^- \ (bicarbamate) \tag{2.2}$$

In comparison, primary and secondary amines have higher affinity for CO_2 and fast reaction. However, primary and secondary amines have higher regeneration cost due to carbamates formation. Formation of bicarbamates cause the tertiary amines requires lower regeneration cost. Although it has low regeneration cost, but the reactions are very slow and exhibit a lower affinity. Hence, primary and secondary amines were advance selected. Nowadays, the technology of catalyst was grown mature. Additional of small amount of activator to such a solution enhances the absorption process (Rajesh et al., 2006).

In this study, primary amines which is monoethanolamine (MEA) was selected to be used in the CO_2 capture process. There are a lot of advantages using MEA for the absorption process. MEA is primary amine which has smaller molecule size compare to other amines which make it easier to react. MEA has very low solvent and it is ease of reclamation. MEA has low absorption of hydrocarbon. This shows that exist of other hydrocarbon would not affect the efficiency of CO_2 capture (Singh, 2011).

2.4 *Molecular dynamic simulations*

Molecular dynamic is a technique for computer simulation of complex systems which modeled at the atomic level. It gives the description of the atomic and molecular interaction that governs microscopic and macroscopic behaviors of physical systems. The connection can be shown in figure 2-5 (Cuendet & Michielin, 2008).

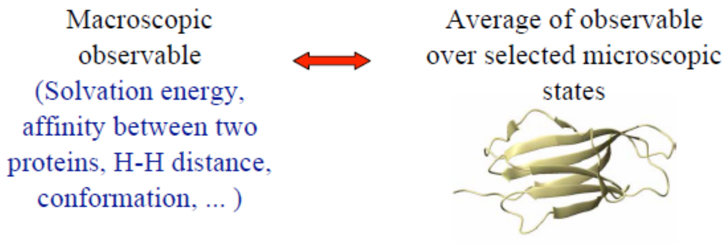

Figure 2-5: Connection between macroscopic world and microscopic world

Molecular Dynamic (MD) simulation depends on time evolution of the system. A microscopic replication of a macroscopic system constructed in a manageable box of molecules to study the configurations of the molecules and properties of the system in future. MD applied an initial configuration of molecules with calculated bond length, bond angle, force applied and other identities of the molecules as input. It is then computes the molecular forces based on the interaction parameter with a given force field. Newton's second law of motion is used to determine the velocities and molecules' position. The law is shown in Equation 2.3.

$$f_i = m_i a_i = m_i \frac{d^2 r_i}{dt^2} \tag{2.3}$$

The mass of the particle *I* is represented m_i, a_i is acceleration, t is time and f_i is the force acting on the particle which also can be calculation through the Equation 2.4 shown below where $V(r_i)$ is the potential energy respect to the particle's position.

$$f_i = \nabla_i V(r_i) \tag{2.4}$$

Data collected from previous proceeding step will be used to calculate new velocities and molecules' position after a very small time interval. MD generates a trajectory of the system with respect to time (Allen & Tildesley, 1987).

2.4.1 Molecular Dynamics Time Integration Algorithm

In MD simulations, Newton's second law of motion is used to calculate the time evolution of a set of interacting particles. From equation 2.3 where r_i in term of t can be express as $r_i(t) = (x_i(t), y_i(t), z_i(t))$. x_i, y_i, and z_i ware the 3 direction of motion for a moving particle.

'Particles' corresponding to atoms, they represent distinct entitles such as chemical group that usually described in terms of interaction law. Integration of Equation 2.3 require information of instantaneous forces on the particle, initial positions and particle velocity to be solved numerically. MD trajectories are defined by both position and velocity vectors which describe the time evolution of the system in phase space. The position and velocities propagates in a finite time interval via numerical integrator. A good example for this is the Verlet, Velocity Verlet and Leapfrog algorithm (Jaroslaw, 2010). Verlet algorithm is the most common to be used in molecular dynamic simulations. Changing of particle position with time defined by $r_i(t)$, whereas the velocities $v_i(t)$ determine the temperature and kinetic energy in the system. The trajectories movement of the particles will be displayed and analysed with averaged properties (Farmahini, 2010).

Verlet algorithm from Taylor expansion is used to calculate the velocity explicitly which may affect the simulation with constant pressure. Modest operation mode and storage are required for velocity of Verlet. This allow the usage of a relatively long time steps duration as the position (r), velocities (v), and acceleration (a) are calculated at the same time with high precision using Equation 2.5.

$$r_i(t+\Delta t) \cong 2r_i(t) - r_i(t-\Delta t) + \frac{F_i(t)}{m_i}\Delta t^2 \tag{2.5}$$

Besides this, the capability to conserve energy with numerically stable and time reversible properties becomes the reason for the software developer to use this algorithm (Farmahini, 2010).

2.4.2 Periodic boundary condition (PBC)

Periodic boundry condition (PBC) can be expressed as a periodic array of simulation boxes in every boxes surrounded by other replicated boxes in all directions. Figure 2-6 illustrate the two-dimensional representation of PBC.

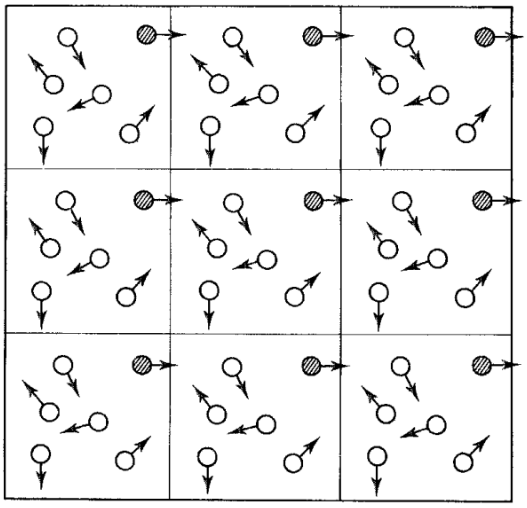

Figure 2-6: 2-D periodic boundary condition (PBC)

PBD is very useful to simulate bulk environment in limited number of molecules. It can be seen from figure 2-6 that if one molecule leaves the simulation box, the same molecule emerges from the opposite side of the box at the same time. Various shapes of PBC can be used in MD simulation. The shape of the periodic boundary condition depends on the configuration of the system. There are 5 shapes of periodic boundary condition to be used in MD simulation since they can fill all the space by translation operation of the central box in three dimensions such as simple cubic box, hexagonal prism, truncated octahedron, rhombic dodecahedron and elongated dodecahedron.

It is very important to decide the box size in the simulation. Simulation always carried out in a box. Hence, an appropriate fit with the dimension of the fluctuation or interaction should be chosen during simulation. As a case in point, short-range L-J interactions can be usually fitted into the boxes larger than on each side but this will be more problematic for long-range interactions (Leach, 2001).

2.4.3 Force fields

In molecular dynamic simulation, it applies the molecular mechanic concept with forces as important elements. Every potential energy functions are required to incorporate into force field concept to become the driving force of simulation. Force field can be divided into 3 generations. First generation generic force field which has a wide coverage to provides reasonable prediction of molecule structure which included all existent forces (Leach, 2001). Second generation improve the prediction quality rather than a wide applications. The third generation force field use quantum mechanical calculation to produces the highest quality prediction which is very similar to actual condition and it can be applied to wide range of disciplines including biochemistry and materials science. Hence, it is important to select the right force field to give significant effect on the simulation result (Balbuena & Seminario, 1999).

In this study, the force field incorporates with both intermolecular and intra-molecular forces. COMPASS (Condensed-phase optimized molecular potentials for atomic simulation studies) is employed to simulate all the systems. This is because COMPASS is categorized as the third generation force field which is suitable in the simulation of organic molecule, inorganic gas molecule and polymers. The simulation qualities can achieve up to nearly same as the industrial process. COMPASS force field is a licensed force field which adds to the cross coupling term for the prediction of vibration frequencies and structural variation (Schlecht, 1998).

2.4.4 Thermodynamic Ensemble

A thermodynamical ensemble is a collection of microscopic states that all realize an identical macroscopic state. A microscopic state of system is given by a point (r, p) of the phase space of the system, where $r = (r_1, ..., r_N)$ and $p = (p_1, ..., p_N)$ are positions and the momenta of the N atoms of the system. There are three type of ensembles usually employed in MD simulations. The first type is NVE ensemble or microcanonical ensemble which fixed the number of particles (N), volume (V) and energy (E). The second type is the NPT or Isobaric-isothermal ensemble where the number of particles (N), pressure (P) and temperature (T) are fixed during the dynamic process through the usage of pressure and temperature controller. The third type is the canonical ensemble (NVT) which allows energy and pressure to be fluctuated (Allen & Tildesley, 1987) and is widely used in biological molecular simulations. Amongst these ensembles, NVE and NPT are the ensembles chosen to be applied in this study.

2.4.4.1 NVE

Equilibrium phase is the phase when the system evolves from the starting configuration to a stable or equilibrium system with energy conservation. In this study, NVE is used during this stage as this ensemble did not permit external forces to the system which is suitable to generate the state point of the system. The equilibrium stage will continue until the values of set monitored properties such as energy become stable, even though there is a possibility of energy drift during the ensemble generated (Rai, 2012).

2.4.4.2 NPT

NPT is chosen for this study as it imitates the experimental condition such as the requirement to have the correct pressure and temperature in the simulation (York, 2007). It is also suitable for large systems. In addition, the simulation under NPT is able to measure the equation of state for the system even if the viral expression for the pressure cannot be evaluated (Frenkel & Smit, 2002). The NPT ensemble has been used by Gunther et al. (2005) to collect the data of predicting the extractability of hydrophilic solutes by modified carbon dioxide extraction technique.

2.4.5 Analysis Parameter

The properties of MD simulations can be categorized into two parts which is the structure properties and dynamic properties. The structural properties are the object of the system which did not depend on time such as radical distribution function (rdf). While the dynamic properties of the system are fluctuate and time dependant properties. It calculates through time specified trajectory data such as mean square displacement (msd). However, this study only concern on the radial distribution function (rdf) as it can be used to give insight on the intermolecular interaction (Adam et al., 2013).

2.4.5.1 Radial distribution function

Radial distribution function (rdf) is an important structural property that basically used to characterize compound in general and Lernnard Jones potential (LJ). In particularly, rdf measure the probability of finding the neighbouring molecules at particular distance r from a reference molecule (Anslyn et al., 2006). Lernnard Jones potential (LJ) used to calculate the interaction potential between a pair of atoms. The rdf has the ability to be expressed in thermodynamic function such as in the internal energy E which is the sum of kinectic and potential energy, U as in Equation 2.6 (Hill, 1960).

$$E = \frac{3}{2}NkT + U \tag{2.6}$$

Integrating the Equation 2.6 will produce the potential energy, U and the equation can be rewritten as Equation 2.7.

$$\frac{E}{NkT} = \frac{3}{2} + \frac{\rho}{2kT}\int_{0}^{\infty} u(r)g(r,\rho,T)4\pi r^{2}\, dr \tag{2.7}$$

The radial distribution function can be defined by the Equation 2.8.

$$g(r) = \frac{1\langle N(r, r + dr)\rangle}{\rho 4\pi r^2 dr} \tag{2.8}$$

Where ρ is the density of atoms, r is the spherical radius, N is the number of atom. The rdf is important for three main reasons. Firstly, it is useful for pairwise additive potentials, knowledge of the rdf is sufficient information to calculate thermodynamic properties, particularly the energy and pressure. Secondly, the rdf is very well developed integral equation theories that permit estimation of the rdf for a given molecular model. Last but not least, the rdf can be measured experimentally, using neutron-scattering techniques. Figure 2-7 shows the schematic explanation of g(r) of a monoatomic fluid. The atom at the origin is highlighted by a black sphere. The dashed regions between the concentric circles indicate which atoms contribute to the first and second coordination number of shells respectively (Adam et al., 2013).

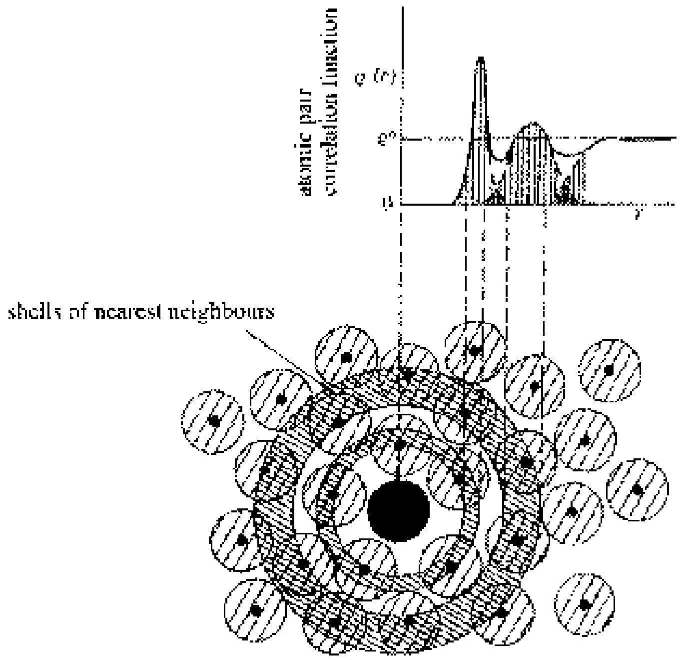

Figure 2-7: Schematic explanation of g(r) of a monoatomic fluid

The g(r) pattern basically depends on the phase of the system. The ideal gas will approach g(r) = 1. These patterns can be seen in Figure 2-7. Figure 2-7 (a) represents the g(r) in gas, (b) in liquid and (c) in solid phase.

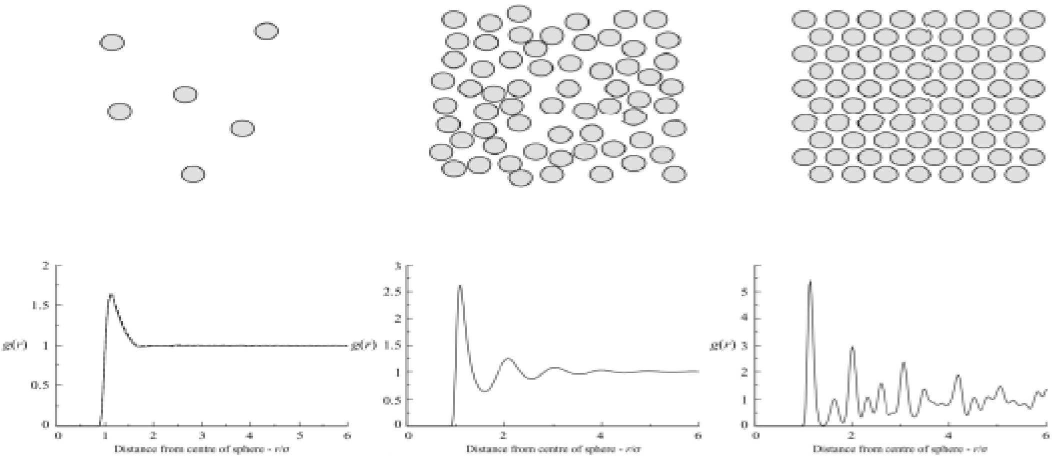

(a) Gas phase (b) Liquid phase (c) Solid phase

Figure 2-8: The atomic configuration and rdf pattern for (a) gas, (b) liquid and (c) solid phase (Barrat & Hansen, 2003)

From Figure 2-8, the rdf pattern for solid phase fluctuates more frequently as compared to liquid and gas phase. According to kinetic molecular theory of matter, the atoms of solid phase are arranged accordingly so they will vibrate constantly. Vibration between the atoms will cause repulsive force against each other. Therefore, many fluctuations occur as shown in Figure 2-8 (c). Since liquid atoms are just arranged closely to each other and gas atoms are far apart from each other, so their rdf patterns are quite stable as compared to solid phase.

2.4.5.2 Molecular Diffusion

Molecular Diffusion can be described as the spread of molecules through random motion. For a molecule M in an environment where viscous force dominates, its diffusion behaviour can be describe by the diffusion equation as below.

$$\frac{\delta}{\delta t} c(r,t) = D\nabla^2 c(r,t) \tag{2.9}$$

where $c(r,t)$ is a function that describes the distribution of probability of finding M in the small distance of the point r at time t. D is the diffusion coefficient and c is the concentration (Wang & Hou, 2012).

Molecular diffusion always related with the mean square displacement. Mean square displacement (MSD) of atoms in a simulation can be easily computed by its definition

$$MSD = \langle |r(t) - r(0)|^2 \rangle \tag{2.10}$$

where $\langle |r(t) - r(0)|^2 \rangle$ are the average distance over all the atoms. Meanwhile MSD consist the information on the atomic diffusivity. If the environment is in liquid state, MSD grows linearly with time. So, it becomes useful to characterize the environment system behaviour in term of slope, which is the diffusion coefficient *D*:

$$D = \lim_{t \to \infty} \left(\frac{1}{6} (\langle |r(t) - r(0)|^2 \rangle) \right) \tag{2.11}$$

Number six in Equation 2.11 indicate the six possible direction of diffusion for atoms when in consideration of three dimensional system. It must be change to four if the system is two dimensional (Furio, 1997). Rearrangement of the equation is then expressed as the equation below:

$$MSD = \lim_{t \to \infty} (6Dt) \tag{2.12}$$

The diffusion coefficient D can be obtained from a plot of the MSD versus time as shown in figure 2-9. The gradient of the line will be the value of $\langle |r(t) - r(0)|^2 \rangle$.Hence, the value of coefficient diffusion, D of a molecule will be the gradient of the graph divided by 6 (Stefan, 2001).

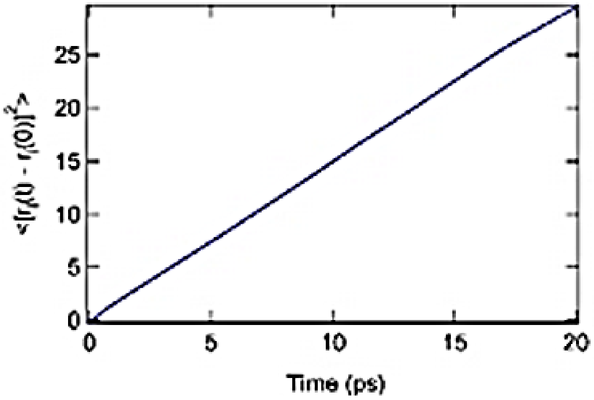

Figure 2-9 graph of MSD versus time

2.5 *Modelling of molecules*

2.5.1 *Introduction*

There are numerous techniques such as membrane separation, chemical solvent separation, cryogenic separation process and physical sorbents separation which are widely used in molecular design technology in chemical, pharmaceutical and agrochemical industries. It plays an important role in molecular simulation because it is necessary for employed molecules and species during simulation.

2.5.2 Intermolecular forces

Intermolecular potential interaction relates to the non-bonded interactions between atoms from different molecules. It occurs between all type of molecules or ions on all state of matter. They range from strong, long distance electrical attractions and repulsion between ions to the relatively weak Van der Waals forces (Margenau & Kestner, 1969). Intermolecular interactions can be categorized into long range and short range interaction which describes how fast they fall off with respect to distance. Electrostatic interactions and Van der Waals interactions are two contributors in this part (Adam et al., 2013).

2.5.2.1 Electrostatic interactions and Ewald summation

Electrostatic interactions are considered as long range interactions which are in group of non-bonded interactions which follow the Coulumb's law. The partial or formal charges (in the ionized molecules) of the atoms cause this type of interactions. Therefore, the mutual potential energy can be expressed and Equation 2.13.

$$U_{AB} = \frac{1}{4\pi\varepsilon_r\varepsilon_0} \cdot \frac{q_A q_B}{R_{AB}} \qquad (2.13)$$

Where ε_0 is vacuum permittivity and ε_r is relative permittivity.

However, electrostatic interactions between all the atoms are not favourable since interactions over very long distances within the periodic boundary condition are negligible. Hence, in order to diminish the computational effort as low as possible and to simultaneously keep the accuracy high enough, the Ewald summation method is introduced. This method is able to calculate the electrostatic energy exactly (Jensen, 2006) and able to include all the effects of long range forces into a computer simulation (Leach, 2001).

Application of Equation 2.14 for all the atom pairs within the periodic boundary condition can be redefined as following (Leach, 2001).

$$U_{el} = \frac{1}{2} \sum_{|n|=0}^{\infty\prime} \sum_{i=1}^{N} \sum_{j=1}^{N} \frac{q_i q_j}{4\pi\varepsilon_0 |r_{ij} + n|} \qquad (2.14)$$

Here a cluster of cubic cells has been assumed so that n is position of the box within the cubic lattice, N is the number of charges in each box and r_{ij} is the minimum distance between charge i and j. The prime on the first sum signifies interactions of $i = j$ are excluded for $n = 0$ which are the interactions between central box and other simulation boxes (Farmahini, 2010).

2.5.2.2 Short range interactions

There are varieties of short range interactions. Those included dipole-dipole, induced dipole and dispersion interactions in combination with the repulsive contribution. Short range interaction is more complex than long range interaction. Electron clouds overlap causes a strong short range repulsive force when electron density and nuclear shielding are reduced. This means the increase in the coulombic repulsion between the positively charged nuclei. This is also the force that prevents a crystal lattice from collapsing itself. However, before nuclear repulsion becomes significant there is is also quantum mechanical effect because the electrons are forced to occupy a smaller portion of space. So, there is a weaker and contrasted longer range attractive interaction at larger interatomic distances arising from the formation of instantaneous dipoles between adjacent electron clouds. This effect is known as the van der waals interaction which is also quantum mechanical in origin (Adam et al., 2013).

Formal charges for lattice simulations and gas surface interactions are non-ionic, thus, the short range potential is the only simulation variable throughout. As such, great care over the form and parameters of the short range interactions must be exercised. It is interesting to note that the long range term makes up the great majority of the total interaction energy. Despite this, by only adjusting the much smaller short range contribution the whole spectrum of crystal structures can be reproduced. Below some of the possible descriptions for the short range interaction are discussed. The most basic form would be a simple harmonic interaction,

$$\Phi_{sr}(r_{ij}) = \frac{1}{2}K(r_{ij} - r_0)^2 \qquad (2.15)$$

where r_{ij} is the distance between two atoms i and j, r_0 is the equilibrium bond distance and K is the harmonic force constant. This model is quite sufficient for systems that only deviate slightly from r_0 and for which interactions can realistically be confined to adjacent pairs of ions. However, for systems where large deviations may be expected (e.g. defective systems) alternative potential forms must be employed.

For example, a Morse potential can be used to describe wider ranges of separation,

$$\Phi_{sr}(r_{ij}) = D_{ij}\left[1 - \exp\left(-\beta_{ij}\{r_{ij} - r_0\}\right)\right]^2 \tag{2.16}$$

where D_{ij} is the disassociation energy of the bond and β_{ij} is a variable parameter that can be determined from spectroscopic data. This type of model is particularly useful in chemical systems to model bonded covalent interactions and the O-H species.

The Lernnard-Jones potential,

$$\Phi_{sr}(r_{ij}) = \frac{A_{ij}}{r_{ij}^{12}} - \frac{B_{ij}}{r_{ij}^{6}} \tag{2.17}$$

where A_{ij} and B_{ij} are the variable attractive and repulsive parameters respectively, is often used to model non-bonded interactions such as rare gas solids. In this form the r^{12} term represents the short range repulsive electron cloud interaction and the r^6 term the intermediate range van der Waals energy.

If the r^{12} term in the Lernnard Jones (LJ) potential is replaced by a more complex dual parameter exponential term the Buckingham potential form results,

$$\Phi_{sr}(r_{ij}) = A_{ij}\exp\left(\frac{-r_{ij}}{\rho_{ij}^{12}}\right) - \frac{C_{ij}}{r_{ij}^{6}} \tag{2.18}$$

where A_{ij} and r_{ij} describe components of the repulsive interaction and C_{ij} describes the attractive interaction. A_{ij} and r_{ij} are thought to relate to the number of electrons and the electron density respectively, while C_{ij} is meant to represent the van der Waals interaction. Here and example of LJ potential for neon atom in figure 2-10.

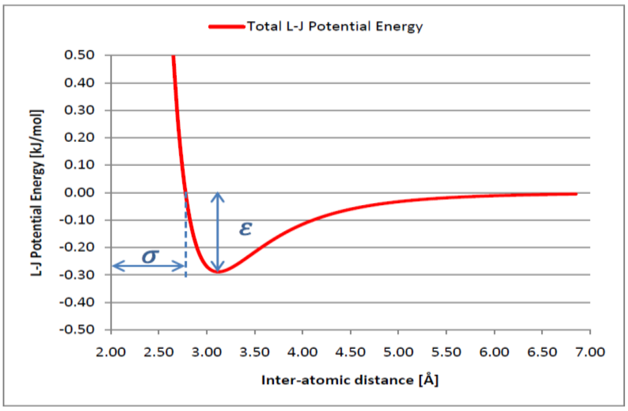

Figure 2-10: Lernnard Jone (LJ) potential energy for Neon atom

In the case where ions have small polarisabilities the *C*-term is often omitted giving rise to a Born-Mayer potential (Hafemeidter & Zahrt, 2004),

$$\Phi_{sr}(r_{ij}) = A_{ij}exp\left(\frac{-r_{ij}}{r_{ij}^{12}}\right) \tag{2.19}$$

The Buckingham and Born-Mayer potentials have been used successfully in the excellent to model a wide range of crystal structures and ionic species.

Finally it is worth mentioning the original simple short range potential for ionic systems (Born & Huang, 1954),

$$\Phi_{sr}(r_{ij}) = \frac{A_{ij}}{r_{ij}^{n}} \tag{2.20}$$

where A_{ij} is a variable parameter and the optimum value of n was determined to be approximately 9.

The classification of the short range interaction used here is somewhat generalised since the van der Waals interaction will operate over several atomic distances. However, it is often convenient to think of it as a short range interaction since it reduces rapidly with r_{ij}. As such, the interaction is often considered zero beyond a sensible cut-off distance.

2.5.2.2.1 Dispersion forces

According to Israelachvili (2011), dispersion forces make up the most important contribution to the total van der waals forces between atoms and molecules. Dispersion force act like the gravitational force between all atoms and molecules. They play a role in a host of important phenomena such as adhesion; surface tension; physical adsorption; wetting; the properties of gases, liquids, and thin films; the strengths of solids; the flocculation of particles in liquids; and the structures of condensed macromolecules such as proteins and polymers. Their main features may be summarized as follows:

1. They are long-range forces and, depending on the situation, can be effective from large distances (greater than 10 nm) down to interatomic spacing (about 0.2 nm).
2. These forces may be repulsive or attractive, and in general the dispersion force between two molecules or large particles does not follow a simple power law.
3. Dispersion forces not only bring molecules together but also tend to mutually align or orient them, though this orienting effect is usually weaker than with dipolar interactions.

4. Dispersion forces are not additive that is the force between two bodies is affected by the presence of other bodies nearby. This is called the non additivity of an interaction.

2.5.3 Intra-molecular forces

Intra-molecular interactions relate to the potential interaction between atoms in every molecule. This includes bond stretching, angle bonding, dihedral motions (torsional rotation) and out of plane (inversion) potentials and Van der Waals interaction between all the atoms which are not separated by three or more covalent bonds (Eloranta, 1973). Intramolecular forces are stronger than intermolecular forces which determine the stability of the molecule. Intramolecular forces are classified into three major bond forces which are namely ionic, covalent and metallic.

In an organic compound, the intramolecular or covalent bond forces will contribute to the bonded energy terms which can be divided into E_{stretch} (bond term), E_{bend} (angle term), $E_{\text{out of plane}}$ (improper dihedral term) and E_{torsion} (torsion term) (Shattuck, 2008). The bond term or E_{strech} is the energy required to stretch the bond from its equilibrium length. The angle term (E_{bend}) is the energy required to bend the bond from its equilibrium angle. The E_{torsion} (torsion term) is the energy needed to rotate the bond. The improper dihedral term or $E_{\text{out of plane}}$ is the energy required to deform a planar group of atom from its equilibrium angle. All of these energy terms are used by the bond in order to resist the changes and revert to their equilibrium position which is of paramount importance during parameterized force field.

2.5.4 Partial atomic charges

Partial atomic charge is very crucial for computing physical, chemical and biological properties, and reactivity of molecules. Information such as atomic charge in a given species must be identified to predict the stability, solvation energetics of various molecules, course a particular reaction, and its interaction between molecules. It is very hard to calculate the partial atomic charges within the molecules. Since the position of electron around atoms are not fixed and other neighbouring atoms continuously affecting the electrons, a simple scheme called Mulliken population analysis (MPA) is introduced to partition the electronic distribution among the atoms based on contribution of atomic orbitals (Mulliken, 1955). However, MPA neglects the effect of electronegativity of various atoms and dependant to the size of basis set (Huzinaga & Sakai et al., 1990).

To avoid the deficiency of MPA such as the problem of non-orthogonality in regards with atomic orbitals. Application of a symmetric orthogonalization scheme named Löwdin population analysis (LPA) is proposed. LPA can be defined by Equation 2.21.

$$N_i = \sum\nolimits_i S_{ii}^{\frac{1}{2}} P_{ii} S_{ii}^{\frac{1}{2}} \tag{2.21}$$

Where N_i is atomic population, P_{ii} is density matrix, S_{ii} is overlap matrix, and $S_{ii}^{\frac{1}{2}} P_{ii} S_{ii}^{\frac{1}{2}}$ is the Löwdin density matrix. MPA and LPA scheme are categorized as class II charge models which molecular wave functions (MO) are partitioned into contributor atomic orbitals (AO). Class I charged model is developed only for neglect of diatomic differential overlap theory. Class III charge model stands for physical observables. This study will focus on class IV charge model which is the combination of class II and class III charge models to provide a more accurate charge distribution.

2.6 Types of Mechanics

There are two type of computational tool to be used in MD simulations which are quantum mechanics (QM) and classical molecular mechanics (MM). QM calculate the electronic structure of a molecule in a more accurate ways but expensive. QM can calculate the forces at a range from 10-100 atoms with 10-100ps (picoseconds). However, MM calculates the empirical forces via Newton's law of motion in a less accurate way but fast. MM calculates forces at a range of 10^4-10^5 atoms with 10-100ns (nanoseconds). The combination of the two computational tools contribute a very accurate dynamic simulation calculation with considered all the forces included. They can compensate for the disadvantages of both. Figure 2-11 shows the electronic structure of a molecule where figure 2-12 shows the empirical forces of molecules.

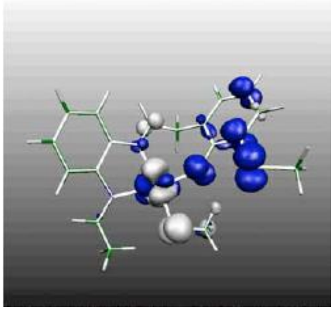

Figure 2-11: Electronic structure of a molecule

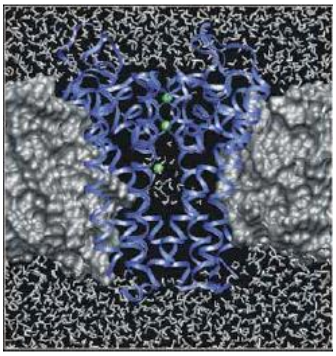

Figure 2-12: Empirical forces of molecules

2.6.1 *Quantum mechanics (QM)*

Quantum mechanics are known as quantum physics and quantum theory. It is a branch of physics which deals with physical phenomena at nanoscopic scales where the action is on the order of the Planck constant. It departs from classical mechanics primarily at the quantum realm of atomic and subatomic length scales. Quantum mechanics provides a mathematical description of much of the dual particle-like and wave-like behaviour and interactions of energy and matter. Quantum mechanics provides a substantially useful framework for many features of the modern periodic table of elements including the behaviour of atoms during chemical bonding and has played a significant role in the development of many modern technologies (Chester & Marvin, 1987). Hence, the state of a system is fully described by the wave function $\Psi(r_1, r_2, \ldots, t)$ which contains information about all the properties of the system that are open to experimental determination (Atkins & Friedman, 2005).

QM is the fifth and final postulate describing time dependent "dynamical evolution of the wave function". This is the called the Schrödinger equation represented by Equation 2.22 as a partial differential equation,

$$i\hbar \frac{\partial \Psi}{\partial t} = H\Psi \tag{2.22}$$

Where H is the Hamiltonian operator corresponding to the total energy of the system and is the reduced Planck's constant. This is equivalent to Equation (2.23) presenting the total kinetic and potential energies explicitly in cartesian coordinate system.

$$i\hbar \frac{\partial \Psi}{\partial t} = -\frac{\hbar^2}{2m} \nabla^2 \Psi + V(x, y, z)\Psi \tag{2.23}$$

Exact solution of the Schrödinger equation for large systems is impossible and for small systems even very complicated. Therefore, another basic concept named atomic orbitals (AO) is introduced. The atomic orbitals are “one-electron wave functions in atoms” labeled by letters s, p, d, f, (...) so that for instance an electron occupying a s-orbital is called s-electron. Similarly for other orbitals there are p-electrons in p-orbitals and so on (Atkins & Friedman, 2005).

If the exact information of wave function Ψ_{nlm_l} is known, the Schrödinger equation can be solved easily where n, l and m_l are called the quantum numbers. These quantum numbers are introduced as below.

n is the principle quantum number ranging from 1, 2, 3… specifying the number of electronic shells on the atomic structure. This number also decides about the energy of the shell according Equation (2.24) and controls range of the l quantum numbers from 0 to $n - 1$.

$$E_n = -\left(\frac{Z^2 \mu e^4}{32\pi^2 \varepsilon_0^2 \hbar^2}\right)\left(\frac{1}{n^2}\right) \tag{2.24}$$

Where Z is the atomic number, μ is reduced mass and is vacuum permittivity.

Each electronic shell is composed of n number of subshells which are the atomic orbitals with quantum number$l$.l is also defined as the orbital angular momentum quantum number giving the orbital angular momentum of the electron through Equation (2.25). Moreover, this quantum number controls the range of between – l and l.

$$Magnitude\ of\ the\ angular\ momentum = \{l(l+1)\}^{\frac{1}{2}}\hbar \tag{2.25}$$

m_l is called magnetic quantum number, and is defined as component of the orbital angular momentum of an electron. This quantum number is represented by individual orbitals so that there are $2l + 1$ individual orbitals in each subshell (Atkins & Friedman, 2005).

2.6.2 Molecular mechanics (MM)

Molecular mechanic was developed out of a need to describe molecular structures and properties in as practical a manner as possible. The applicability of molecular mechanics includes molecules containing thousands of atoms and thermodynamic and kinetic properties.

Molecular mechanics methods are based on the following principles:

i. Nuclei and electrons are lumped into atom-like particles.
ii. Atom-like particles are spherical (radii obtained from measurements or theory) and have a net charge (obtained from theory).
iii. Interactions are based on springs and classical potentials.
iv. Interactions must be preassigned to specific sets of atoms.
v. Interactions determine the spatial distribution of atom-like particles and their energies.

In Molecular mechanics, molecule is just like a system of rigid balls that are connected via springs. The molecule geometry will be affected by non-bonded interactions (Hehre, 2003),compared to those bonded or intramolecular interactions. This ideal geometry of the molecules has its steric energy or energy due to the molecule's geometry or calculated by Equation 2.26.Steric energy is the energy of the molecules which the inherent form of energy between the real molecules and the relative forms.

$$E_{\text{steric energy}} = E_{\text{stretch}} + E_{\text{bend}} + E_{\text{strech-bend}} + E_{\text{out of plane}} + E_{\text{torsion}} + E_{\text{van der waal}} + E_{\text{qoulumbic}} \qquad (2.26)$$

The steric energy can be classified into two main types of interactions which is intramolecular and intermolecular. The first 5 energy terms from Equation 2.26 are under intermolecular interaction while the last 2 are the intramolecular energy terms (Adam et al., 2013).

3 METHODOLOGY

3.1 MD simulations methods

MD simulation is an essential technique to study a variety of molecular properties including molecular diffusion. Diffusion process not only can be study in atomic details, but also under various thermodynamic conditions that is unreachable by experiments. In this study, molecular dynamic simulation will be used to simulate and study the intermolecular interactions between the molecules in MEA the absorption process. The MD simulation has the ability to enable the insight into the intermolecular interactions during the absorption process.

To replicate the behaviour of the system closed to the real industry situation, speciation of the system needs to be determined accurately. Related component speciation will be specified accordingly from the literature review which can be used as the initial composition of the system included monoethanolamine (MEA), carbon dioxide (CO_2), and carbamate ion (Chakraborty, 1988). Figure 3-1 is an example of a MEA molecule after speciation.

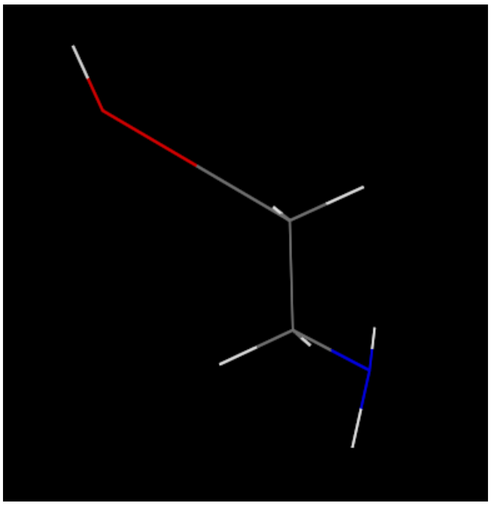

Figure 3-1: A speciated MEA molecule

After the speciation of the system is determined, modelling of the decided species will be started using Molecular Dynamic (MD) technique of the specified species for the solution. Procedure of this technique involves three main steps. The steps include all interaction parameter have to decide through a suitable force field, then geometry optimization of the molecule and lastly the calculation of partial charges. Molecular

Dynamic (MD) technique was used to investigate the molecular distribution of the system inside the absorption solution (Hinchliffe, 2000).

In order to perform the MD simulation in this study, the simulation box will be divided into two different parts. One part will be occupied by liquid phase which including the monoethanolamine and another box will fill with gases compound (CO_2). The two boxes will bring into contact with each other and form a gas-liquid interface to allow the absorption process to take place across the interface surface (Belonoshko, 1998). Before that, simulation box of pure molecules (pure MEA, pure water, and pure CO_2), binary system (MEA+CO_2, CO_2+H_2O and MEA+H_2O) is created to study the behaviour of each molecules before absorption process occur. Figure 3-2 shows the simulation box of a pure MEA at 45^0C.

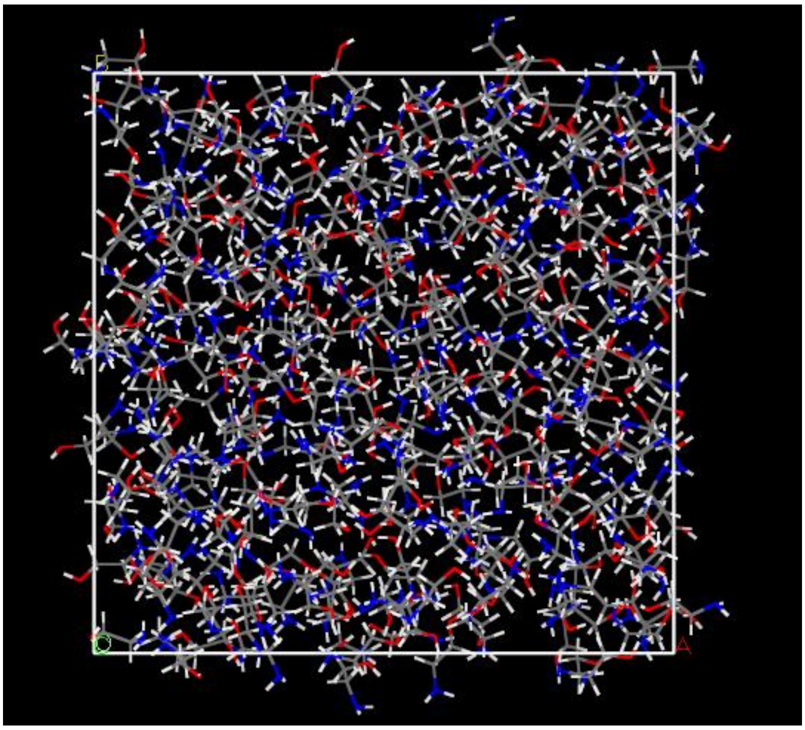

Figure 3-2: The simulated box construction of pure MEA

Thermodynamic conditions of the system will be set in the MD simulation of the system closed to real absorption process comditions. The thermodynamic conditions under NVE (constant number of moles, volume and energy), NPT (constant number of moles, pressures and temperature) and NVT (constant number of moles, volume and temperature) are assembled up to 5ns. The movement of every molecule will be integrated according to the Newton's Second Law of motion to achieve the equilibrium (Keffer & Baig et al., 2005).

This study investigated the molecular structure effect on solvent properties such as functional group on solvent properties like basicity and amine group during the absorption process (Ebenso et al., 1999). The simulation results are interpreted in terms of radical distribution function and diffusion coefficient. The MD simulation procedure study is summarized in figure 3-3.

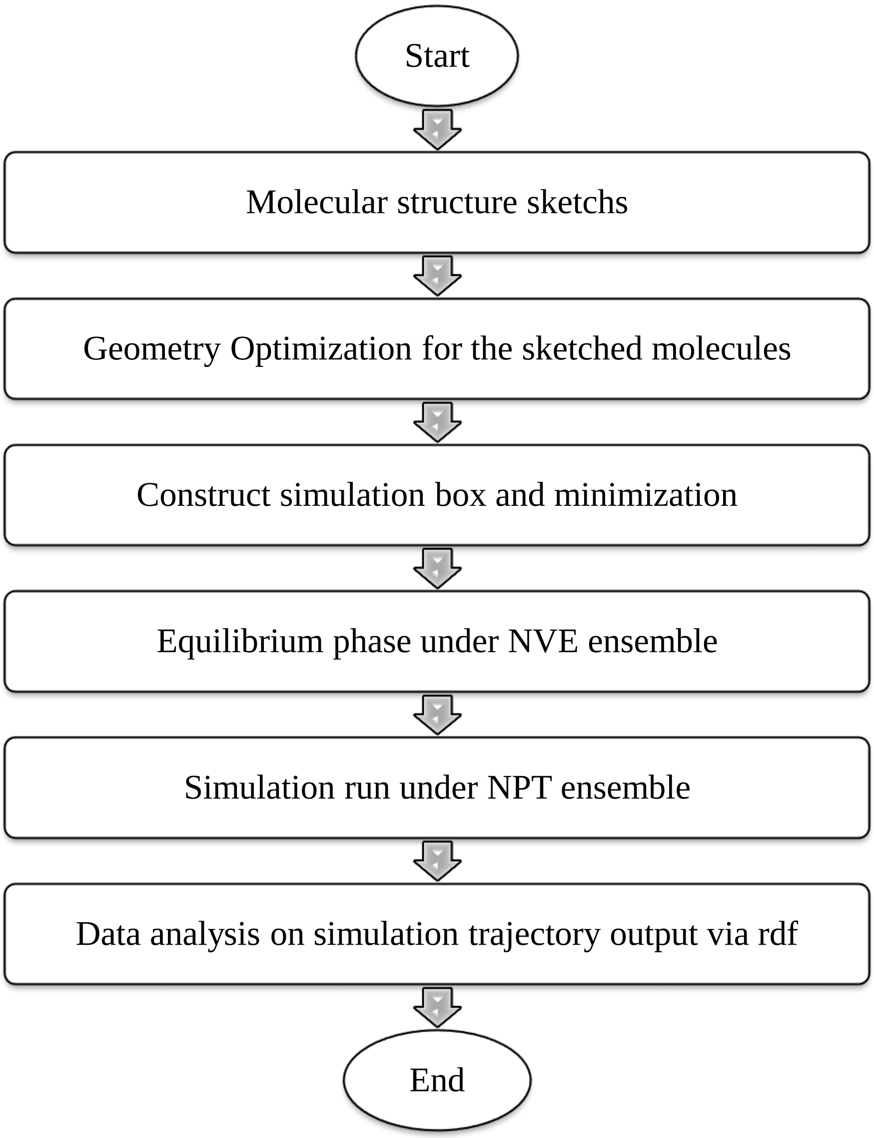

Figure 3-3: Summarization of MD simulation procedure

3.2 Software

In this study, the process simulation is performed using Materials studio software package version 4.4 (Grillo et al., 2004). It is a very useful tool to comprehend and reveal the intermolecular interaction between molecules during the absorption process. The acid gas used in this study is carbon dioxide and the solvent is monoethanolamine (MEA). By applying Newton's second law, the dynamic aspect of the system will be simulated and the coordinate system will be used to calculate radial distribution function (rdf) (Anslyn at al. 2006), and diffusion coefficient. This will be used to shows how strong the molecule interaction and even which atoms of the molecules attracted the most between the solvent and acid gas (Matteoli & Mansoori, 1995).

4 RESULTS AND DISCUSSIONS

The intermolecular interaction using rdf graph shows the interaction between molecules before reaction mechanism of absorption occur. The results obtained from this study present the potential interaction of molecules or the physical interaction between molecules. Meanwhile it also determines the strength of the molecular force and movement of each molecule. 3D boxes are generated to identify the position of each molecule while interactions occur as shown in figure 3-3.

4.1 Radial Distribution function analysis

4.1.1 Primary system

Three stages of simulation are established to study the intermolecular interaction of MEA absorption for CO_2 capture. The first stage name primary system involved a single molecule. Molecular simulation for carbon dioxide is conducted at temperature 45 °C. Figure 4-1 shows the atomic structure of carbon dioxide, where -C3 indicate the carbon atom, -O1 and -O2 indicate the first and second oxygen atom, respectively. The similar notation applied for water and monoethanolamine molecule as shown in figure 4-2 and figure 4-3, respectively.

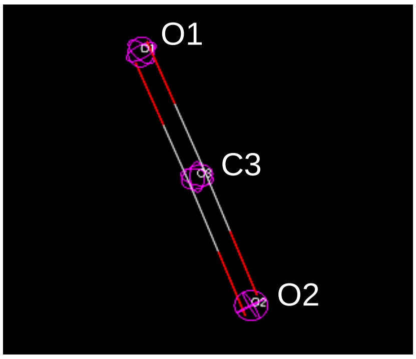

Figure 4-1: Atomic structure of carbon dioxide.

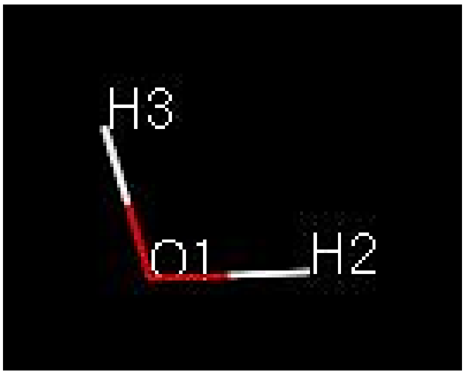

Figure 4-2: Atomic structure of water

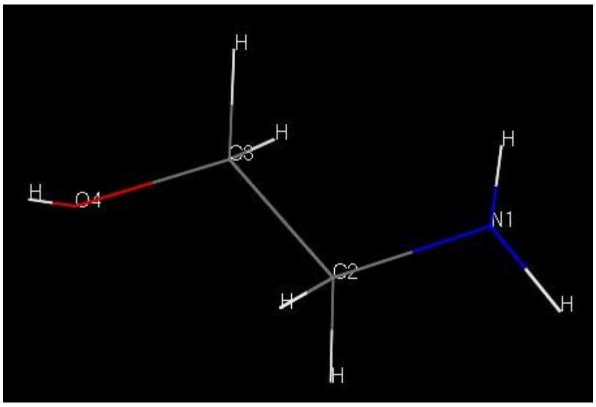

Figure 4-3: Atomic structure of monoethanolamine

4.1.1.1 *Carbon dioxide and water*

From figure 4-4, g(r) is the radius of gyration (root mean square distance of the objects' parts from its center of gravity) and (Å) is the forces between molecules or atoms. From this figure, it shows that the strongest intermolecular interaction occurred at 4.75 and 5 Å between the carbon atom (C3) and second oxygen atom (O2)(see red line). The greater the value of Å means the greater the interaction between the molecules.

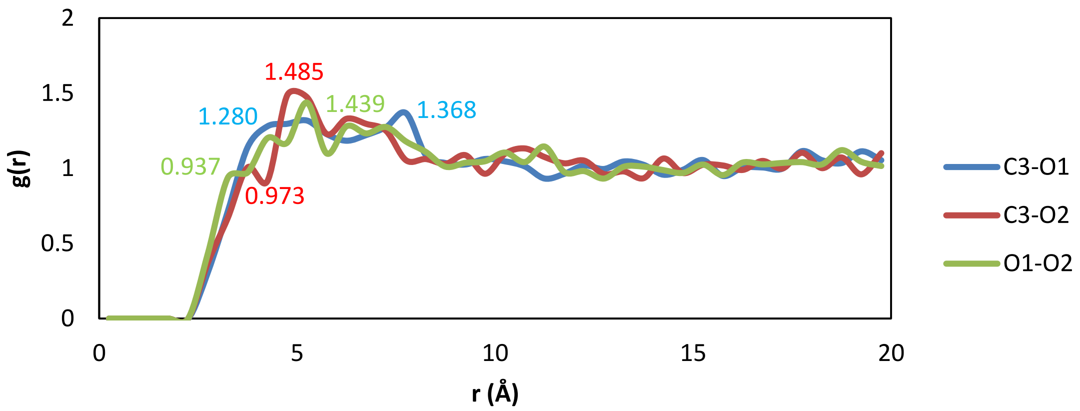

Figure 4-4: Molecule interaction in pure CO_2 molecules at 45^0C.

At a very small distance, r, the function g(r) was essentially zero since the atoms cannot strongly overlap their electronic shells. By referring C3—O1 interaction (blue colour line), it reached the first peak at 4.75 but the highest peak was found at 7.75 Å. This means that there was a potential interaction which is 1.280 at r = 4.25 Å. The g(r) value appears to be at the highest peak, 1.368 at r = 7.75 Å which indicates the highest potential distance, r for the molecules to interact with each other. At long distance, the trend line of interaction would reach the value of g (r) ≈ 1 which indicates there is no long range order and the molecular interaction almost negligible. The trend line for plot in Figure 4.4 shows some fluctuations closed to one at distance greater than 10 Å. Table 4-1 shows the data of function g(r) peak of different molecule interaction.

Table 4-1: RDF of pure CO_2 at 45^0C.

Type of interactions	First peak	Highest peak
C3—O1	1.280	1.368
C3—O2	0.973	1.485
O1—O2	0.937	1.439

From figure 4-3, the pattern trend line of CO_2 at 40^0C has less fluctuation compared to 45^0C. From table 4-1 and 4-2, the first potential interaction of CO_2 at 40^0C is always higher then CO_2 at 45^0C. As from the C3—O1 interactions, CO_2 at 40^0C has 1.4963 times to occur interactions between two atoms than CO_2 at 45^0C which is only 1.280 times for the interactions to occur.

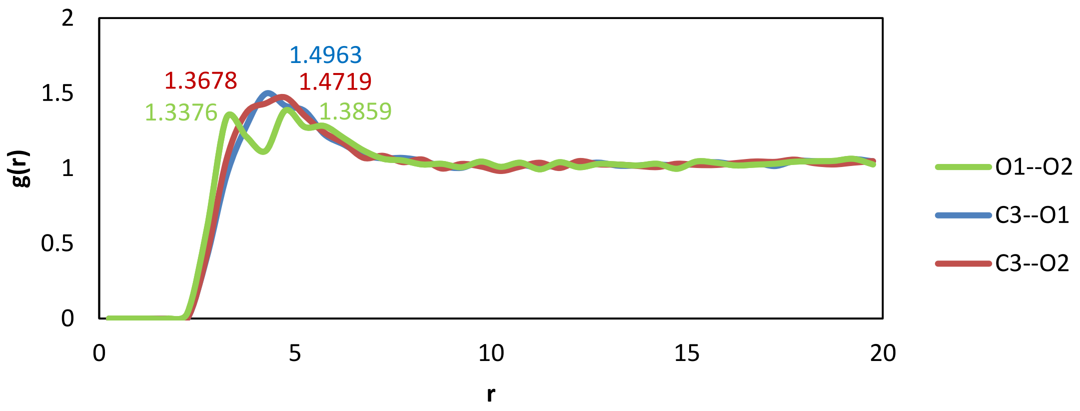

Figure 4-5: Molecule interaction in pure CO2 molecules at 40^0C.

Table 4-2: RDF of pure CO_2 at 40^0C.

Type of interactions	First peak	Highest peak
C3—O1	1.496	1.496
C3—O2	1.368	1.472
O1—O2	1.338	1.386

As the temperature increases, the kinetic energy of the molecule will increase. Collision of the molecules will occur more frequently and causes higher repulsive force which results the distance between two molecules to increase. The molecules become loose. Hence, carbon dioxide at 40^0C always has a higher g(r) value than 45^0C.

The intermolecular interaction for water as shown in figure 4-6 shows that the first interaction occur at distance 1.75 Å for O1-H3 and O1-H2 interactions which indicate the presence of hydrogen bonding in water. Since the interaction between O and H is the same strength and distance for water molecules, hence the rdf for O1-H3 and O1-H2 are said to be identical to each other.

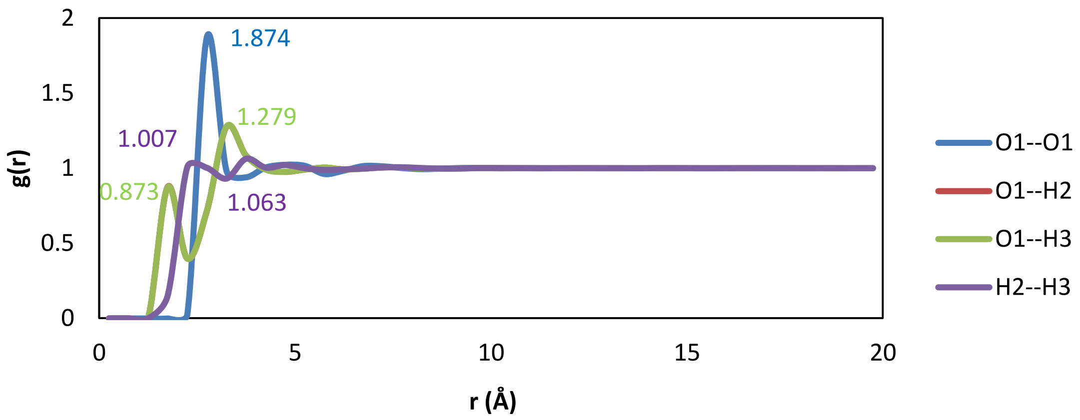

Figure 4-6: Molecule interaction in pure H_2O molecules at 45^0C

Table 4-3: RDF of pure H_2O at 45^0C.

Type of interactions	First peak	Highest peak
O1—O1	1.874	1.874
O1—H2	0.873	1.279
O1—H3	0.873	1.279
H2—H3	1.007	1.063

As shown in figure 4-6 and figure 4-7, the interaction of O1—O1 has the highest peak but the interaction of H2—H3 has the lowest peak. Oxygen atom is highly electronegative but hydrogen atom is highly electropositive. Two highly electronegative oxygen atom interacting creates a highly repulsive force. So, this is the reason the probability of O1—O1 interaction to occur is the highest. The trend of molecular interaction for H_2O was almost the same for both temperatures. The line O1—H2 interaction has the same Angstrom value and function g (r) with O1—H3 for both temperatures of 40^oC and 45^oC. Hence, the effect of temperature on the interaction was not significant for H_2O. The trend of molecular interaction for H_2O at 40^oC as shown in figure 4-7 is similar with 45^oC. The temperature range used in this study keep the water remain in liquid phase and results similar pattern observed in this study. The trend rapidly damped, showing the gradual smearing out of short-range order of water.

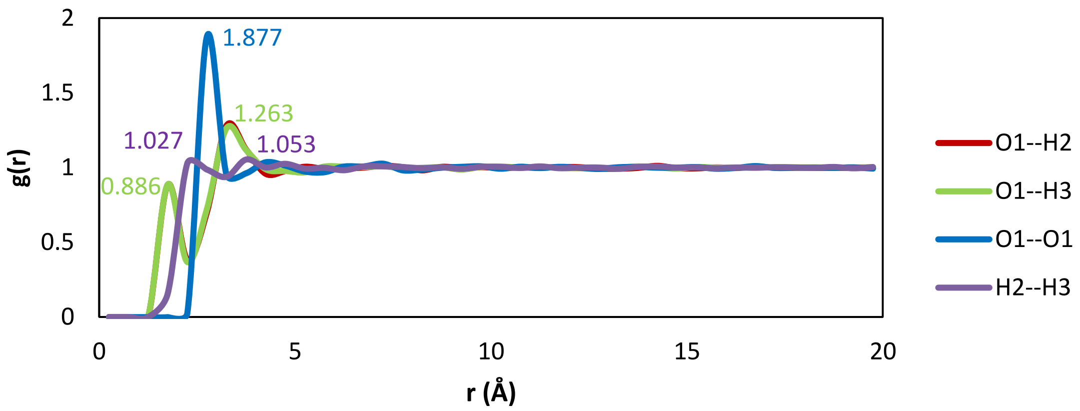

Figure 4-7: Molecule interaction in pure H_2O molecules at 40^0C.

Table 4-4: RDF of pure H_2O at 40^0C.

Type of interactions	First peak	Highest peak
O1—O1	1.877	1.877
O1—H2	0.886	1.263
O1—H3	0.886	1.263
H2—H3	1.027	1.053

4.1.1.2 Monoethanolamine

The interaction between monoethanolamine molecules is analysed at temperature 40^oC and 45^oC. As can be seen from figure 4-8, the interaction between oxygen atom of molecule MEA with hydrogen atom from hydroxyl group,-OH of molecule MEA is higher than amino group of molecule MEA, -NH. This is due to the polar bond between –OH groups of monoethanolamine. Since –OH band has two lone pairs at oxygen atom, while –NH bond has only one lone pair. Hence, -OH bond is more polar than –NH bond. Then, -OH bond has higher tendency to form hydrogen bonding with water molecules compare to –NH bond.

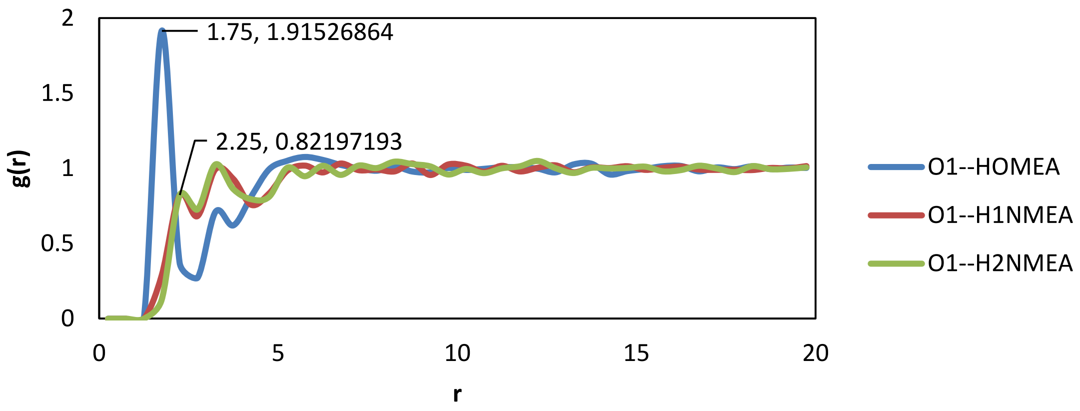

Figure 4-8: Molecule interaction based on –OH in pure MEA molecules at 40°C

The strength of the interaction is summarized in Table 4-5.

Table 4-5: RDF of pure MEA at 40^{0}C.

Type of interactions	First peak	Highest peak
O1—OH$_{MEA}$	1.75	1.915
O1—H1N$_{MEA}$	2.25	0.82
O1—H2N$_{MEA}$	2.25	0.82

Primary system just considered the molecular interaction for single component. It is expected that this interaction will change for binary and tertiary system which considered the molecular interaction with different component. Hence, analysis on primary system does not give insight on how the absorption process will occur. So, further analysis on binary system and tertiary system is carried out and discussed in the following sections to give more insight on absorption process.

4.1.2 Binary system

Molecular simulation for binary system consists of MEA and H_2O molecules. The interactions of nitrogen and oxygen atoms of MEA and hydrogen atom in H_2O were analysed through characterization of radial distribution function (RDF). The results shown in figure 4-9, show the interaction between amino group, -NH and hydroxyl group, -OH with water. Similar intermolecular interaction is observed for f O1MEA-H2H2O and

O1MEA-H3H2O while interaction of N1MEA-H2H2O is similar with N1MEA-H3H2O. These identical interactions show that the position of –H bond in water does not affect the intermolecular interaction between –NH and –OH with H atom of water. As can be seen from this graph,–OH group of MEA has stronger interaction with water compared to –NH group. The first interaction between amino group with the closed neighbouring water occur at 1.75 Å with g(r) value, 0.809 while for –OH group has g(r) value, 0.507. The stronger interaction of –OH group with water is due to the hydrogen bonding.

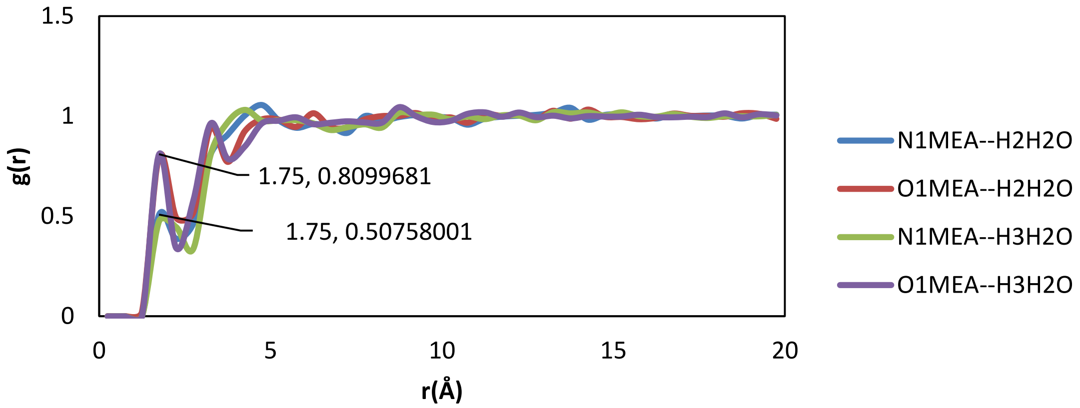

Figure 4-9: Molecular interaction in binary system (MEA +H_2O) at 40°C

There are two electrical interactions covalent between atoms and Van der Waals, there exists an intermediate interaction called the “hydrogen bond” or “H-bond”. It occurs between a molecular group, most often OH or NH that carries an H-atom and exhibits a marked electric dipole moment, and the O- or N-atom of another molecule. Most H-bonds XHY are formed between two independent molecules X-H and Y. These are “intermolecular H-bonds” and when speaking of H-bonds in the following with no other specification, one always refers to this type of H-bond, which represents the large majority of them. Another category of H-bonds however exists, the “intramolecular H-bonds”, where molecular groups XH and Y are both parts of a same molecule. Even if they represent only a minority of H-bonds, these intramolecular H-bonds include quite a large variety of H-bonds. These two types of H-bonds have macroscopic manifestations that are different: an intramolecular H-bond involves a single molecule, whereas an intermolecular H-bond involves two molecules that become independent upon disruption of the H-bond. H-bonds may be characterized by various quantities such as their enthalpies of formation or their XY equilibrium distance, or, better, the wavenumbers of the centers of some of their characteristic spectral bands. For binary system, the studies focus on the hydrogen bonding of water and –OH group of MEA since it was proved that the –NH group of MEA has weak interaction with Hydrogen bonding of water for temperature at 40°C. By analysis of figure 4-10 (25°C), figure 4-9 (40°C), and figure 4-11 (45°C), stronger interaction was observed at 45°C compare to at 25°C and 40°C. The g(r) value for hydrogen bonding is 0.82, 0.81 and 0.97 with respect to temperature of 25°C, 40°C and 45°C. The binary system's data is a necessary as a reference and interpretation for tertiary system.

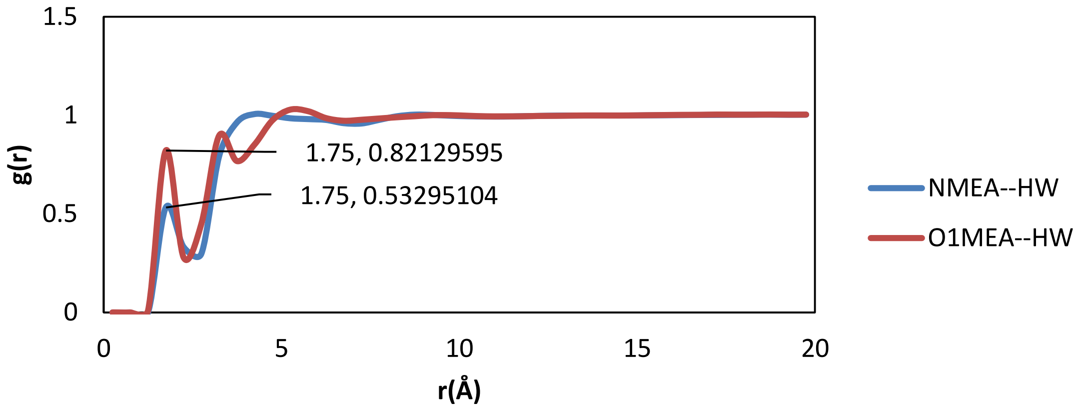

Figure 4-10: Molecular interaction in binary system (MEA +H2O) at 25°C

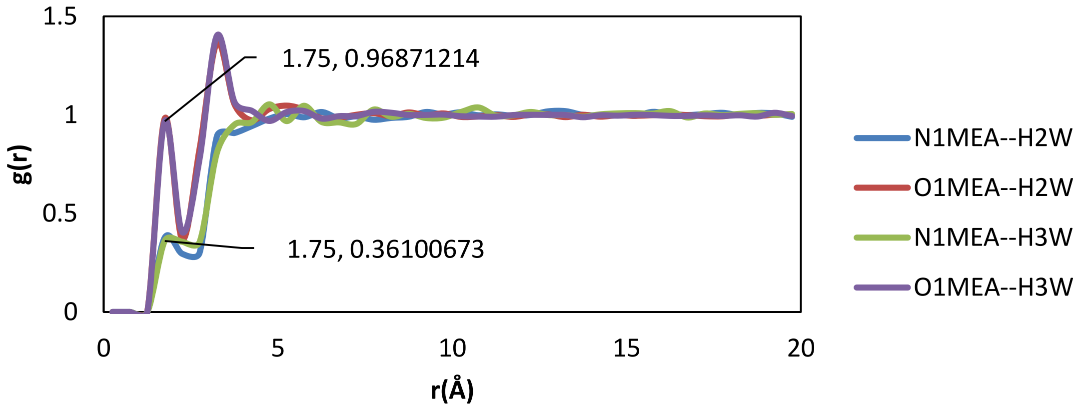

Figure 4-11: Molecular interaction in binary system (MEA +H2O) at 45°C

Table 4-6 lists the value of r and g(r) for significant intermolecular interaction observed from figure 4-9 at different temperature.

Table 4-6: RDF of binary system at 25°C, 40°C and 45°C.

Temperature (°C)	N_{MEA}-H_{H2O}		O_{MEA}-H_{H2O}	
	r(Å)	g(r)	r(Å)	g(r)
25	1.75	0.53	1.75	0.82
40	1.75	0.50	1.75	0.81
45	1.75	0.36	1.75	0.97

4.1.3 Tertiary system

As shown in figure 4-12, a strong intermolecular interaction between water molecule and –OH group of MEA (see red line) is observed. At the distance of r = 1.75Å , the trend HO_{MEA}-O_{H2O} has the highest peak of g(r) = 2.049. In comparison with the intermolecular interaction of HN_{MEA}-O_{H2O} (see blue line), the strongest interaction is observed at longer distance r = 3.25 and the g(r) is 1.027 which is lower than HO_{MEA}-O_{H2O}. This has clearly explain that the –NH group of MEA has less possibility to interact with water molecule.

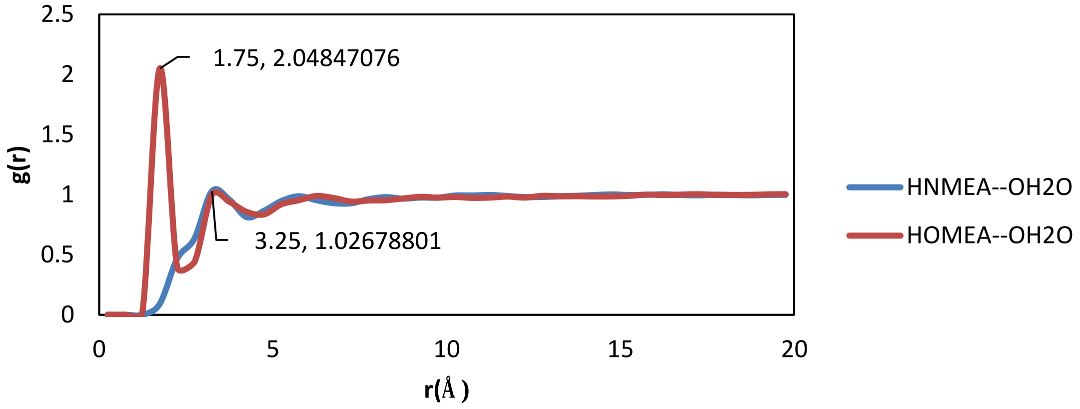

Figure 4-12: Molecular interaction between MEA and H_2O in tertiary system at 40°C

As shown in figure 4-13, it was found that CO_2 has stronger interaction with –NH group of MEA compare to –OH group of MEA. Radial distribution function plot of CO_2 shows that –NH group of MEA has g(r) = 1.226 with distance of r = 4.25 while –OH group has g(r) = 0.946 with a distance of r = 3.75. Higher number of g(r) represent higher number of molecule in that particular shell of number r(Å). From the observation of figure 4-12 and figure 4-13, it is concluded that CO_2 is more attractive to –NH group of MEA molecule. This physical interaction of –NH group of MEA molecule with CO_2 is the initial step for the chemical reaction to occur during the absorption process to form carbamate ions while H_2O that is more attractive with –OH group of MEA to form a hydrogen bonding which increase the solubility of MEA in water.

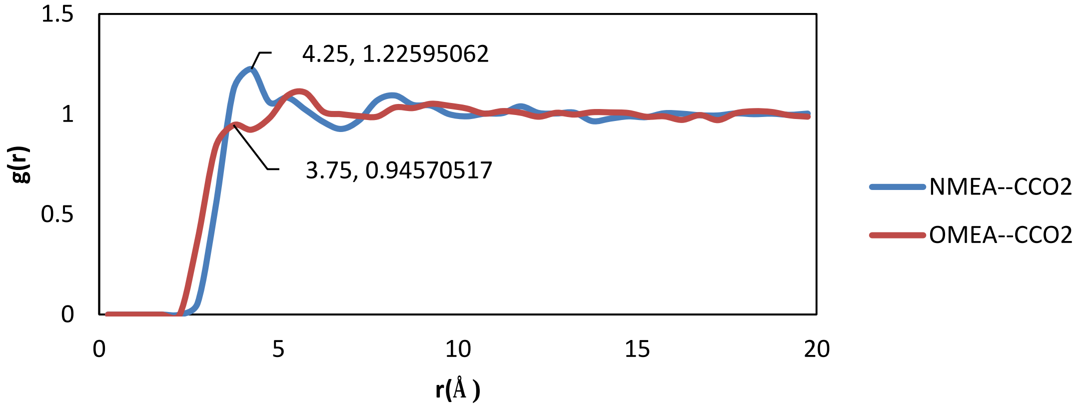

Figure 4-13: Molecular interaction between MEA and CO_2 in tertiary system at 40°C

During absorption process, CO_2 react with MEA to form carbamate ions through zwitterion reaction mechanism. The equation is shown below (Kim et al, 2013).

$$2\,\mathrm{NH_2(C_2H_4OH)} + \mathrm{CO_2} \leftrightarrow \mathrm{(C_2H_4OH)NHCOO^-} + \mathrm{(C_2H_4OH)NH_3^+} \tag{4-1}$$

$$\mathrm{(C_2H_4OH)NHCOO^-} + H_2O \leftrightarrow RNH_2 + HCO_3^- \tag{4-2}$$

From equation 4-1, it is proven that the reaction mechanism of CO_2 react with –NH group of MEA and H_2O attracted by the –OH group of MEA.

By referring figure 4-12 to figure 4-15, the g(r) values of OH_{MEA}-O_{H2O} (red line) for tertiary system are 1.56, 2.04 and 2.29 at temperature of 25°C, 40°C and 45°C respectively. Since MEA molecule has two polar group which are polar amino group and polar hydroxyl group, the probability to find the first neighbor atom of hydrogen bond (HO_{MEA}-O_{H2O}) in tertiary system is higher compared to binary system. Hydrogen bond has significant influence in solubility of MEA in water and affects the CO_2 absorption reaction in aqueous MEA solution. MEA play as a weak base dissolve in H_2O then neutralizes acidic compound which produce ionic compound. In primary amine, the carbamate ion will form. It is observed that the intermolecular interaction strength of OH_{MEA}-O_{H2O} is increased as the temperature increased. The similar behaviour is observed for binary system.

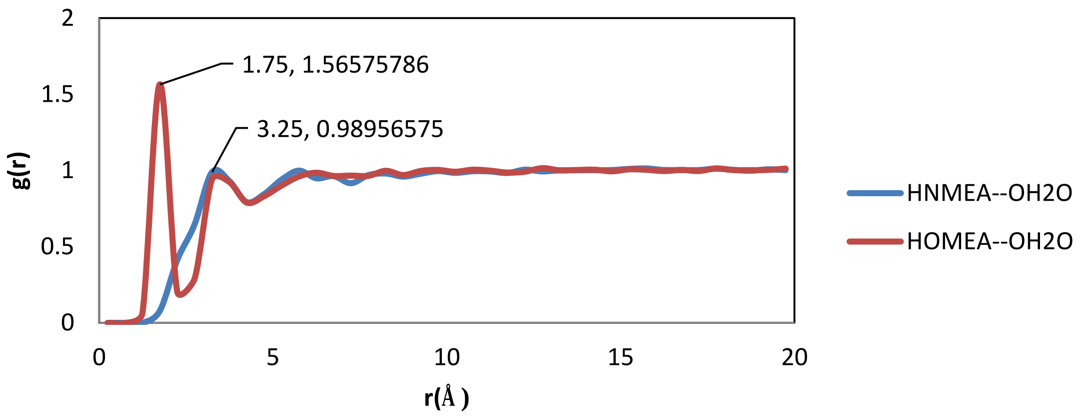

Figure 4-14: Molecular interaction between MEA and H_2O during absorption at 25°C

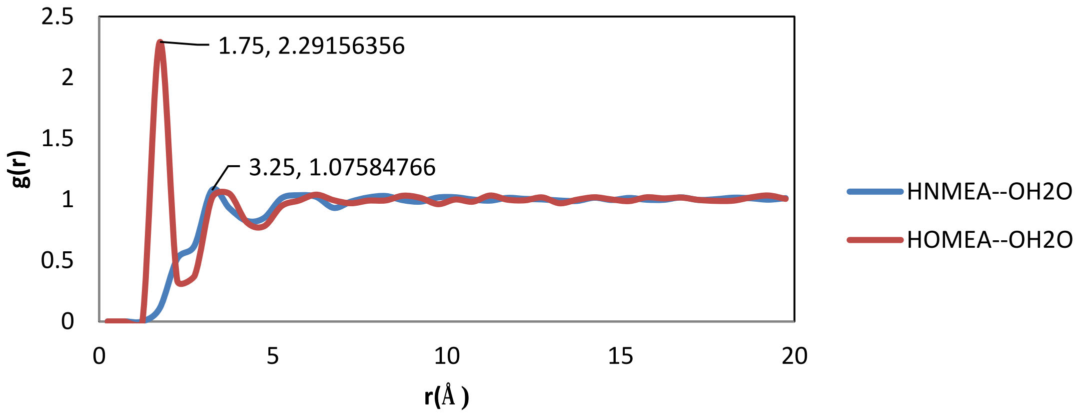

Figure 4-15: Molecular interaction between MEA and H_2O during absorption at 45°C

As depicted in figure 4-13 to figure 4-17, it was known that the g(r) value of N_{MEA}-C_{CO2} for tertiary system is 1.23, 1.54 and 1.3 with respect to temperature at 40°C, 25°C and 45°C. All the three figure shows a higher intensity of interaction between CO_2 and –NH group of MEA. This significantly contribute to the zwitterion and carbamate reaction.

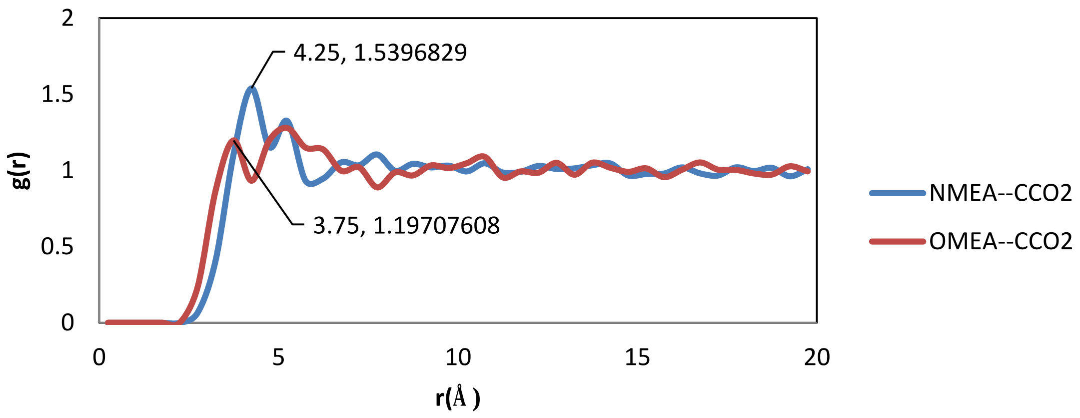

Figure 4-16: Molecular interaction between MEA and CO_2 in tertiary system at 25°C

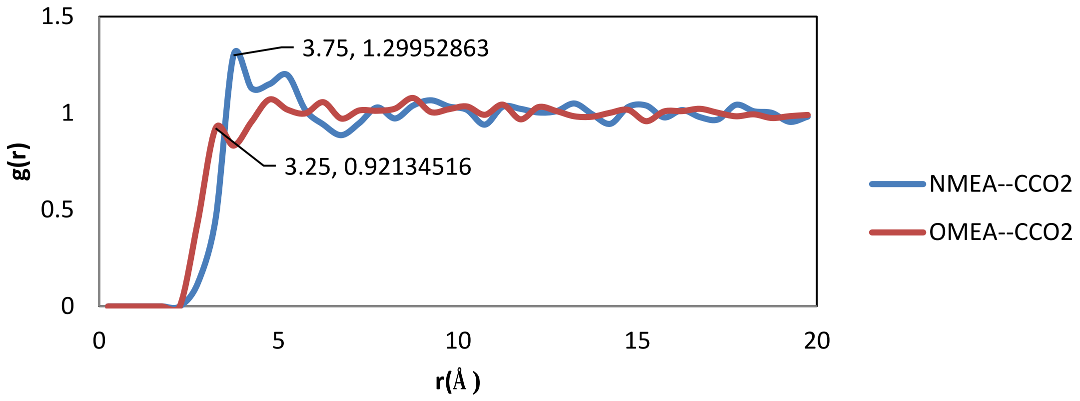

Figure 4-17: Molecular interaction between MEA and CO_2 in tertiary system at 45°C

As a summary, the data collected from tertiary system which included from figure 4-12 until figure 4-17. The data can be interpret into Table 4-7 as below.

Table 4-7 : RDF of Tertiary system at 25°C, 40°C and 45°C

Temperature (°C)	HN_{MEA}-O_{H2O}		HO_{MEA}-O_{H2O}	
	r(Å)	g(r)	r(Å)	g(r)
25	3.25	0.99	1.75	1.56
40	3.25	1.03	1.75	2.04
45	3.25	1.08	1.75	2.29
	HN_{MEA}-C_{CO2}		HO_{MEA}-C_{CO2}	
25	4.25	1.54	3.75	1.20
40	4.25	1.23	3.75	0.95
45	3.75	1.30	3.25	0.92

4.2 *Mean Square Displacement*

The motion of an individual molecule in a dense fluid does not follow a simple path. As it travels, the molecule is jostled by collisions with other molecules which prevent it from following a straight line. This relationship can be written as $<r^2> = 6Dt$.

As shown in figure 4-18, the plot is not linear at beginning of times. This is because the path a molecule takes will be an approximate straight line until it collides with its neighbour. Only when it starts the collision process will its path start to resemble a random walk. Until it makes that first collision, we may say it moves with approximately constant velocity, which means the distance it travels is proportional to time, and its MSD is therefore proportional to the time squared. Thus at very short time, the MSD resembles a parabola. This is of course a simplification - the collision between molecules is not like the collision between two pebbles, it is not instantaneous in space or time, but is `spread out' a little in both. This means that the behaviour of the MSD at short time is sometimes more complicated than this MSD plot shows.

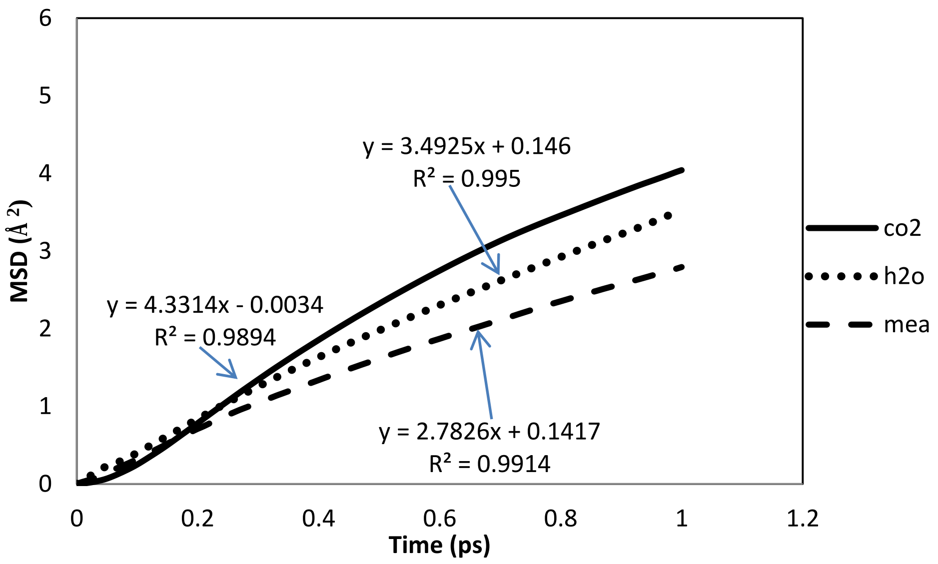

Figure 4-18: MSD graph at 25°C

The linear (straight line) dependence of the MSD plot is apparent. If the slope of this plot is taken, the diffusion coefficient, D may be readily obtained.

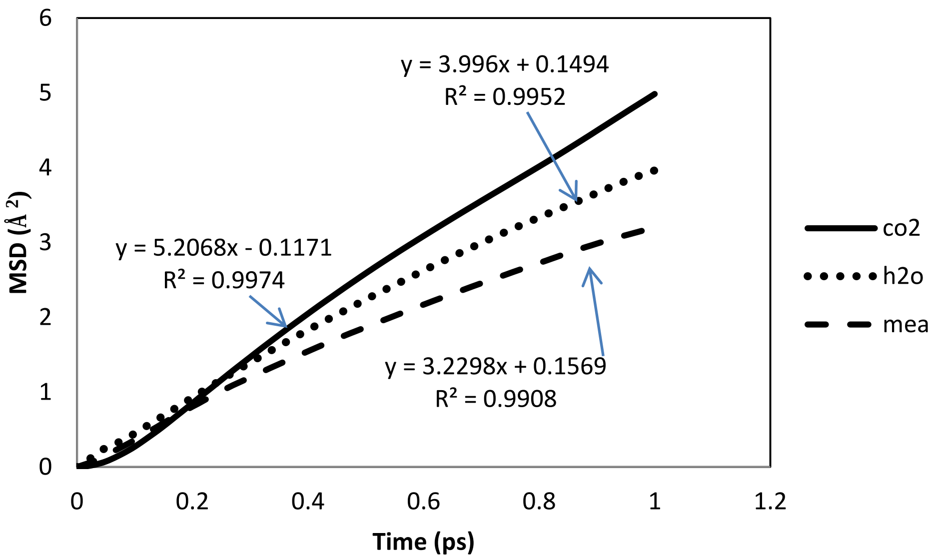

Figure 4-19: MSD graph at 40°C

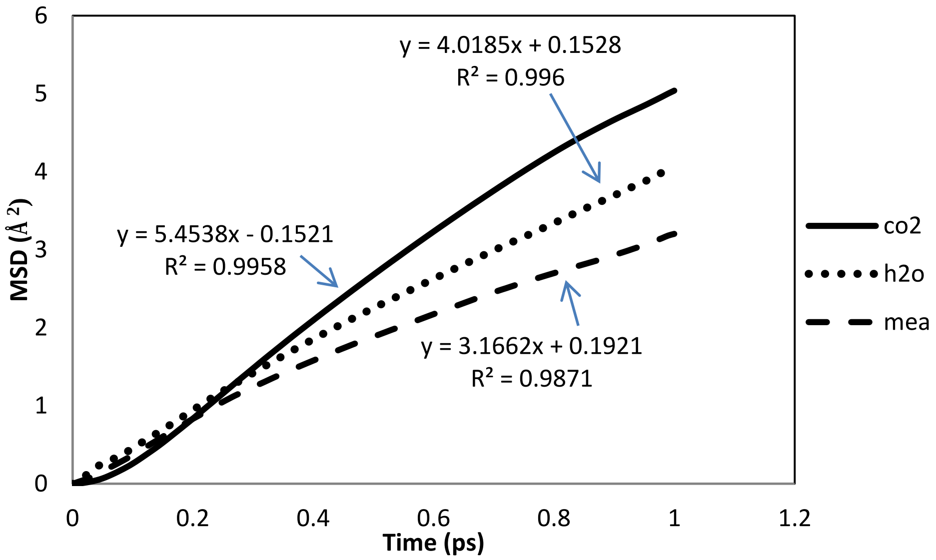

Figure 4-20: MSD graph at 45°C

From Figure 4-18, Figure 4-19, and Figure 4-20, gradient of each line represent the MSD/t of each molecule. Hence, the MSD/t of each molecule at different temperature is shown Table 4-8.

Table 4-8: MSD/t of each molecule at different temperature.

Molecule	MSD/t (Å ^{2}/ps)		
	25 ^oC	40 ^oC	45 ^oC
CO_2	4.3314	5.2068	5.4538
H_2O	3.4925	3.9960	4.0185
MEA	2.7826	3.2298	3.1662

Since D is equal to MSD/t divided by six as shown in equation 2-12 with proper unit conversion the D of each molecule at different temperature can be concluded as in Table 4-9.

Table 4-9 : Diffusion coefficient of each molecule at different temperature

Molecule	D (m^2/s)		
	25 ^oC	40 ^oC	45 ^oC
CO_2	$7.2189e-9$	$8.6781e-9$	$9.0897e-9$
H_2O	$5.8208e-9$	$6.6600e-9$	$6.6975e-9$
MEA	$4.6378e-9$	$5.3553e-9$	$5.2769e-9$

Due to the size of molecule, it is found that the CO_2 diffuse faster than MEA in water. Besides that, it is found that the diffusion coefficient of each molecule increase with temperature. With a higher reactivity of molecules when increasing temperature it is believe the molecule will also diffuse faster. When the molecules diffuse faster, the chance for molecules to colliding and recolliding with each other will increase. Hence the MSD value increased.

5 CONCLUSIONS

5.1 Conclusion

Intermolecular interaction study on monoethanolamine (MEA) absorption process for carbon dioxide capture via molecular dynamic simulation technique is performed at temperature of 25^{o}C, 40^{o}C and 45^{o}C. The results show that the physical interaction between CO2, MEA and water molecule is increased as temperature increased. CO2 has stronger interaction with –NH group of MEA compare to –OH group of MEA due to the existence of hydrogen bonding with –OH group of MEA and water molecules. Hydrogen bond is found to have significant influence on the solubility of MEA in water and affects the CO2 absorption reaction in aqueous MEA solution.

The interaction of –NH group of MEA molecule with CO_2 is the initial step for the chemical reaction to occur during the absorption process to form carbamate ions while H_2O that is more attractive with –OH group of MEA to form a hydrogen bonding which increase the solubility of MEA in water. However, this study concerns the interactions occur before absorption of carbon dioxide.

In regards of molecular diffusion, a study on Mean Square Displacement is carried out. It is found that the diffusion coefficient of each molecule increase with temperature. Higher reactivity of molecules was observed when increasing temperature which results higher diffusivity. When the molecules diffuse faster, the chance for molecules to colliding and recolliding with each other will increase. Hence the MSD value is increased.

5.2 Future Work

Future works for this research can be carried out at a longer simulations time (longer than 5 nanosecond) in order to get better results. A longer simulations time calculates the intermolecular interaction between molecules and behaviour of the molecules more comprehensively.

Besides, the molecular modelling part of this study should be extended. Current study only employed temperature effects on intermolecular interaction before absorption of CO_2 occur. Other ionic species of the reaction during absorption should be included.

This is especially relevant if various thermodynamic conditions or different CO_2 loading factors are going to apply in further simulations. This is because different thermodynamic conditions can change the reaction rate and consequently lead to variation of molecular concentrations (Farmahini, 2010).

Other than that, Hydrogen bond evaluation can be carried out by using an alternative technique such as energetic definition hydrogen bonding rather than geometrical definition which used in this study. Investigation of hydrogen bond based on energetic definition provides useful information about dynamics of hydrogen bonds by calculating pair interaction energy between molecules by means of MD simulations (Chowdhuri & Chandra, 2002)

6 References

Adam, F., Siti Hana, A. B., Mashitah, M. Y., & Tajuddin, S. N. (2013). Molecular Dynamic Simulation of the Patchouli Oil Extraction Process. *Journal pf Chemical & Engineering Data*.

Alie, C. F. (2004). Integrating the Absorption Process and Steam Cycle of an Existing Coal-Fired Power Plant. *CO2 Capture With MEA*.

Allen, M. P., & Tildesley, D. J. (1987). *Computer simulation of liquids.* New York: Oxford University Press.

Anslyn, E. V., & Dougherty, D. A. (2006). *Modern physical organic chemistry.* USA: University Science Book.

Anusha, K. (2010). *Carbon Dioxide Capture by Chemical Absorption: A Solvent Comparison Study.* Mumbai: Massachusetts Institute of Technology.

Atkins, P. W., & Friedman, R. S. (2005). *Molecular Quantum Mechanics.* New York: Oxford University Press.

Balbuena, P., & Seminario, J. M. (1999). *Molecular Dynamics.* Amsterdam: Elsevier.

Barrat, J. L., & Hansen, J. P. (2003). *Basic concepts for simple and complex liquids.* United Kingdom: Cambridge University Press.

Belonoshko, A. B. (1998). Melting of corundum using conventional and two-phase molecular dynamic simulation method. *Physics And Chemistry Of Minerals,* 138-141.

Born, M., & Huang, K. (1954). *Dynamical Theory of Crystal Lattices (1st ed.).* Oxford: Clarendon Press.

Chakraborty, A. K., Bischoff, K. B., Astarita, G., & Damewood, J. R. (1988). Molecular orbital approach to substituent effects in amine-CO2 interactions. *Journal of the American CHemical Society*.

Chester, & Marvin. (1987). *Primer of Quantum Mechanics.* John Wiley.

Chowdhuri, S., & Chandra, A. (2002). *Hydrogen bonds in aqueous electrolyte solutions: Statistics and gynamics based on both geometric and energetic criteria.* Physical Review.

Cuendet, Michel, A., & Oliver, M. (2008). Protein-Protein Interaction Investigated by Steered Molecular Dynamics: The TCR-pMHC Complex. *Biophysical Journal*, 3575-3590.

Ebenso, E. E., Ekpe, U. J., Ita, B., Offiong, O. E., & Ibok, U. J. (1999). Effect of molecular structure on the efficiency of amides and thiosemicarbazones used for corrosion inhibition of mild steel in hydrochloric acid. *Materials Chemistry And Physics*, 79-90.

Eloranta, J. (1973). *Intramolecular dipole reorientation of amino compounds and their interaction with solvent molecules.* Oulu: University Of Oulu.

Energy Information Administration. (2007). *Electric Power Annual 2007 : A Summary.* Washington, D. C.

Energy Information Administration. (2013). *International energy outlook 2013 with projections to 2040.*

Farmahini, A. H. (2010). *Molecular Dynamics Simulation Studies of Piperazine Activated MDEA Absorption Solution with Methane and Carbon Dioxide.* Bergen: The University of Bergen.

Frenkel, D., & Smit, B. (2002). *Understanding Molecular Simulations. From Algorithms to Applications.* California: Academic Press.

Furio, E. (1997). *Mean Square Displacement.* Italy.

Grillo, M., Andzelm , J., Govind, N., Fitzgerald, G., & Stark, K. (2004). Computational Materials Science with Materials Studio: Applications in Catalysis. *Springer*, 207-221.

Günther, M., Maus, M., Wagner, K. G., & Schmidt, P. C. (2005). Hydrophilic solutes in modified carbon dioxide extraction-prediction of the extractability using molecular dynamic simulation. *European journal of pharmaceutical sciences : official journal of the European Federation for Pharmaceutical Sciences*.

Hafemeidter, D., & Zahrt, J. (2004). Exchange-Charge-Model Calculation of the Born—Mayer Repulsive Potential in Ionic Gases and Crystals. *The Journal Of Chemical Physics*, 1428-1437.

Hehre, W. J. (2003). *A guide to molecular mechanics and quantum chemical calculations.* California: Wavefunction, Inc.

Hill, T. L. (1960). *An introduction to statistical thermodynamics.* New York: Dover Publication Inc.

Hinchliffe, A. (2000). *Modelling molecular structures.* New York: John Wiley.

Huzinaga, S., Sakai, Y., Miyoshi, E., & Narita, S. (1990). Extended Mulliken electron population analysis. *The Journal Of Chemical Physics*, 3319-3325.

Israelachvili, J. (2011). *Intermolecular and surface forces (3st ed.).* Amsterdam: Elsevier Academic.

Jaroslaw, M. (2010). *Molecular Dynamics.* Nicholas Copernicus University, Torun, Poland.

Jensen, F. (2006). *Introduction to Computational Chemistry.* West Sussex: John Wiley & Sons Ltd.

Jha, A. R. (2006). *Cryogenic technology and applications.* Amsterdam: Elsevier Academic Press.

Keffer, D. J., Baig, C., Edwards, B., & Adhangale, P. (2005). *A hamiltonian-based algorithm for rigorous molecular dynamics simulation in the NVE NVT, NPT, and NPH ensembles.* American Institute of Chemical Engineers.

Kim, Y. E., Lim, J. A., Jeong, S. K., Yoon, Y. I., Bae, S. T., & Nam, S. C. (2013). Comparison of Carbon Dioxide Absorption in Aqueous MEA, DEA, TEA, and AMP Solutions. *Bulletin of the Korean Chemical Society*, 783-787.

Leach, A. R. (2001). *Molecular modelling.* Harlow, England: Prentice Hall.

Margenau, H., & Kestner, N. R. (1969). *Theory of intermolecular forces.* Oxford: Pergamon Press.

Matteoli, E., & Mansoori, G. A. (1995). A simple expression for radial distribution functions of pure fluids and mixtures. *The Journal Of Chemical Physics*, 4672-4677.

Mulliken, R. S. (1955). Electronic Population Analysis on LCAO[Single Bond]MO Molecular Wave Functions. I. *The Journal of Chemical Physics*, 1833-1840.

Nathalie, J. M., Penderd, v. E., Peter , W. D., Sylvie, F., & Geert, F. V. (2012). *Kinetics of Absorption of Carbon Dioxide in Aqueous MDEA Solutions with Carbonic Anhydrase ar 298 K.*

Park, J. Y., & Yoon, S. J. (2006). Effect of Steric Hindrance on Carbon Dioxide Absorption into New Amine Solutions: Thermodynamic and spectroscopic Verification through Solubility and NMR Analysis. *Environmental Science Technology*, 1670-1675.

Rackley, S. A. (2010). *Carbon capture and storage.* Amsterdam: Butterworth-Heinemann,Elsevier.

Rai, B. (2012). *Molecular modeling for the design of novel performance chemicals and materials.* Florida: CRC Press.

Rajesh, A. K., Chuang, S. C., Soong, Y., & Gray, M. (2006). Thermal and Chemical Stability of Regenerable Solid Amine Sorbent for CO2 Capture. *Energy and Fuels*.

Rubin, E., & De Coninck, H. (2005). *IPCC special report on carbon dioxide capture and storage.* Cambridge, UK: Working Group III Of The Intergovernmental Panel On Climate Change Intergovernmental Panel On Climate Change.

Sada, E., Kumazawa, H., & Butt, M. (1976). Gas absorption with consecutive chemical reaction: absorption of carbon dioxide into aqueous amine solutions. *The Canadian Journal Of Chemical Engineering*, 421-424.

Schlecht, M. F. (1998). *Molecular modeling on the PC.* New York: Wiley.

Shattuck, T. W. (2008). *Molecular mechanics tutorial introduction.* Colby College.

Shrikar Chakravarti, Amitabh Gupta, & Balazs Hunek. (2001). Advanced Technology for the Capture of Carbon Dioxide. *First National Conference on Carbon Sequestration*.

Singh, P. (2011). *Amine based solvent for CO2 absorption.* Enschede: University of Twente.

Stefan, F. (2001). *Reduced Pressure, Energy and Density.*

Wang, J. M., & Hou, T. J. (2012). Diffusion Coefficient. *Application of Molecular Dynamics Simulations in Molecular Property Prediction II*, 3505-3519.

Wessner, C. W. (2009). *An assessment of the SBIR program at the National Aeronautics and Space Administration.* Washington, D. C.: National Academies Press.

York, W. M. (2007). *Unrestrained molecular dynamic simulations of human lysosomal glycoslasparaginase in aqueous solution: A structural study of some mutations of highly conserved mammalian residues.* USA: University of North Carolina.

Young, D. M., & Crowell, A. D. (1962). *Physical adsorption of gases.* London: Butterworths.

Yu, C., Huang, C., & Tan, C. (2012). A review of CO2 capture by absorption and adsorption. *Aerosol Air Qual.*, 745-769.

Yu, L., & Liu, J. (2009). Molecular dynamic simulation study of carbon dioxide-water binary mixtures. *Journal Of Southwest University For Nationalities (Natural Science Edition)*, 42.

Zakkour, P., & Cook, G. (2010). CCS Roadmap for Industry: High-purity CO2 sources. *Sectoral Assessment-Final Draft Report. Global Technology Roadmap For CCS In Industry*.